J|A|C|S
ARTICLES

Published on Web 04/08/2008

EP-2104R: A Fibrin-Specific Gadolinium-Based MRI Contrast Agent for Detection of Thrombus

Kirsten Overoye-Chan,[†] Steffi Koerner,[†] Richard J. Looby,[†] Andrew F. Kolodziej,[†] Stephan G. Zech,[†] Qing Deng,[†] Jaclyn M. Chasse,[†] Thomas J. McMurry,[†] and Peter Caravan[‡,*]

EPIX Pharmaceuticals, 4 Maguire Road, Lexington, Massachusetts 02421, and Athinoula A. Martinos Center for Biomedical Imaging, Department of Radiology, Massachusetts General Hospital, Charlestown, Massachusetts 02429

Received February 1, 2008; E-mail: caravan@nmr.mgh.harvard.edu

Abstract: Thrombus (blood clot) is implicated in a number of life threatening diseases, e.g., heart attack, stroke, pulmonary embolism. EP-2104R is an MRI contrast agent designed to detect thrombus by binding to the protein fibrin, present in all thrombi. EP-2104R comprises an 11 amino acid peptide derivatized with 2 GdDOTA-like moieties at both the C- and N-terminus of the peptide (4 Gd in total). EP-2104R was synthesized by a mixture of solid phase and solution techniques. The La(III) analogue was characterized by and 1D and 2D NMR spectroscopy and was found to have the expected structure. EP-2104R was found to be significantly more inert to Gd(III) loss than commercial contrast agents. At the most extreme conditions tested (pH 3, 60 °C, 96 hrs), less than 10% of Gd was removed from EP-2104R by a challenge with a DTPA based ligand, while the commercial contrast agents equilibrated within minutes to hours. EP-2104R binds equally to two sites on human fibrin ($K_d = 1.7 \pm 0.5$ μM) and has a similar affinity to mouse, rat, rabbit, pig, and dog fibrin. EP-2104R has excellent specificity for fibrin over fibrinogen (over 100-fold) and for fibrin over serum albumin (over 1000-fold). The relaxivity of EP-2104R bound to fibrin at 37 °C and 1.4 T was 71.4 mM^{-1} s^{-1} per molecule of EP-2104R (17.4 per Gd), about 25 times higher than that of GdDOTA measured under the same conditions. Strong fibrin binding, fibrin selectivity, and high molecular relaxivity enable EP-2104R to detect blood clots in vivo.

1. Introduction

Thrombosis is the underlying pathology in a number of cardiovascular diseases which affect millions worldwide. Heart attack, ischemic stroke, pulmonary embolism, and deep vein thrombosis all have culprit blood clots (thrombi). Thrombosis can also occur in the cardiac chambers. For example, atrial fibrillation patients are at high risk for atrial thrombosis and the presence of thrombus impacts their treatment. Another area of intense research is vulnerable atherosclerotic plaque, where unstable lesions can rupture leading to thrombosis and possibly heart attack or stroke. In all of these diseases, there is clearly a need to detect thrombus and to monitor its presence or absence during treatment.

Many imaging techniques are used to identify thrombus, and the preferred technique often depends on the anatomical region. For instance ultrasound is often used to identify deep vein thrombi, while spiral computed tomography (CT) is increasingly used to detect pulmonary emboli. The underlying physics of the different techniques are such that one technique is not ideally suited for thrombus detection in all vascular territories. As a result, there has been an effort to develop imaging probes that specifically delineate thrombus pathology. Different approaches have been taken to design thrombus-specific probes, and this is perhaps not surprising given the complexity of the clotting process.[1] The coagulation enzymes thrombin and Factor XIII, the glycoprotein GPIIB/IIIA receptor on activated platelets, and the fibrin polymer have all been exploited as imaging targets.

In the clotting process,[1] platelets become activated and adhere to the vessel wall and each other to form a plug. The enzyme thrombin cleaves the fibrinopeptides on circulating fibrinogen protein enabling end-to-end polymerization of the fibrinogen moieties to produce fibrin. The fibrin mesh is stabilized by cross-links introduced by the enzyme Factor XIII. Activated platelets, fibrin, thrombin, and Factor XIII have all served as targets for imaging agents. In the 1990s several groups[2–7] used technetium-99m labeled peptides or peptidomimetic agonists for the GPIIb/IIIa receptor on activated platelets as a marker of thrombus.

[†] EPIX Pharmaceuticals.
[‡] Massachusetts General Hospital and Harvard Medical School.

(1) Monroe, D. M.; Hoffman, M. *Arterioscler. Thromb. Vasc. Biol.* **2006**, *26*, 41–8.
(2) Barrett, J. A.; Crocker, A. C.; Damphousse, D. J.; Heminway, S. J.; Liu, S.; Edwards, D. S.; Lazewatsky, J. L.; Kagan, M.; Mazaika, T. J.; Carroll, T. R. *Bioconjugate Chem.* **1997**, *8*, 155–60.
(3) Ben-Haim, S.; Kahn, D.; Weiner, G. J.; Madsen, M. T.; Waxman, A. D.; Williams, C. M.; Clarke-Pearson, D. L.; Coleman, R. E.; Maguire, R. T. *Nucl. Med. Biol.* **1994**, *21*, 131–42.
(4) Francesconi, L. C.; Zheng, Y.; Bartis, J.; Blumenstein, M.; Costello, C.; De Rosch, M. A. *Inorg. Chem.* **2004**, *43*, 2867–75.
(5) Lister-James, J.; Knight, L. C.; Maurer, A. H.; Bush, L. R.; Moyer, B. R.; Dean, R. T. *J. Nucl. Med.* **1996**, *37*, 775–81.
(6) Lister-James, J.; Vallabhajosula, S.; Moyer, B. R.; Pearson, D. A.; McBride, B. J.; De Rosch, M. A.; Bush, L. R.; Machac, J.; Dean, R. T. *J. Nucl. Med.* **1997**, *38*, 105–11.
(7) Mitchel, J.; Waters, D.; Lai, T.; White, M.; Alberghini, T.; Salloum, A.; Knibbs, D.; Li, D.; Heller, G. V. *Circulation* **2000**, *101*, 1643–6.

One Tc-based agent was eventually approved for imaging deep vein thrombosis. Jaffer, Tung and co-workers reported near-infrared probes that had specificity for thrombin,[8,9] Factor XIII,[10–12] or activated platelets.[13] Recently, a phage display study against clotted plasma identified peptides that target the fibrin-fibronectin complex in clots. [14]

Both nuclear and optical probes have very good detection sensitivity. A key limitation of nuclear imaging, however, is its relatively poor spatial resolution and the need to have a high target/background ratio. For near-IR imaging, current technology is limited by tissue penetration and scatter. Magnetic resonance imaging (MRI) has excellent spatial resolution and no ionizing radiation and can image deep tissues. MRI has an added advantage of providing anatomical information to put the location of the thrombus in context, e.g., is it in an artery or vein and in which vessel precisely? A positive contrast (bright spot) thrombus imaging agent for use with MRI would be a powerful tool to faciliate a definitive diagnosis and could offer the potential for whole body exams to pinpoint the source of thrombus. However the challenge for MRI agents is sensitivity: for gadolinium-based agents, micromolar concentrations are required in order to generate robust image contrast.[15]

Particle-based technologies provide one means of delivering large numbers of gadolinium chelates to facilitate thrombus imaging. Wickline, Lanza and co-workers developed a platform technology based on a perfluorocarbon emulsion for both MRI[16–18] and ultrasound[19] contrast agents. They could incorporate gadolinium chelates into the emulsion via lipophilic chains on the chelates resulting in thousands of gadolinium ions per particle. They then linked a fibrin specific antibody to the particle and used this to image thrombus in canine models of disease.[16]

We took an alternate approach to designing a fibrin-specific MRI contrast agent. We reasoned that fibrin could be a useful target for a relatively small MRI probe because of its micromolar concentration. In addition, fibrin is present in all thrombi: arterial, venous, and cardiac, but is not found in plasma, thus providing specificity for the thrombus pathology. Moreover, unlike platelets and enzymes, fibrin is accessible in all active stages of clot development. We developed a peptide-based agent called EP-2104R that was targeted to fibrin, providing specificity, and contained four gadolinium chelates to enhance the MRI signal. EP-2104R was found to be effective at providing positive contrast enhancement in preclinical models of carotid artery,[20] coronary artery,[21,22] atrial,[23] and cerebral venous sinus[24] thrombosis as well as models of pulmonary embolism.[22,25,26] The compound proved efficacious in acute (fresh clot) as well as chronic (aged clot) models of thrombosis. A related, analogous compound, EP-1873 was demonstrated to selectively enhance ruptured atherosclerotic plaques in an animal model.[27] EP-2104R differs primarily from EP-1873 in the type of Gd chelator used: a more kinetically inert DOTA-like chelator is used in EP-2104R compared to a DTPA derivative used in EP-1873. Based on these and other studies, EP-2104R was advanced into clinical trials where preliminary results have been promising.[28,29]

Existing clinical MRI contrast agents are markers of extracellular space or provide tissue (blood vessels, liver) specificity.[30] EP-2104R represents a new class of MRI contrast agents, one in which a specific protein is imaged. This advancement beyond anatomical imaging down to the molecular level has been termed molecular imaging.[31] In this report, the synthesis and characterization of the first MRI molecular imaging agent to advance into human trials, EP-2104R, is described. The paramagnetic compound is characterized by a number of analytical methods; in addition NMR studies on the diamagnetic La(III) analogue confirm the expected structure. The kinetic inertness with respect to gadolinium loss, a critical parameter for patient safety, is addressed in a series of competition experiments. The affinity of EP-2104R for human fibrin is described as well as its specificity for fibrin compared to fibrinogen or other plasma proteins. Finally, the NMR relaxation enhancing properties of EP-2104R are also described in different media and over a range of magnetic fields.

(8) Jaffer, F. A.; Tung, C. H.; Gerszten, R. E.; Weissleder, R. *Arterioscler. Thromb. Vasc. Biol.* **2002**, *22*, 1929–35.
(9) Tung, C. H.; Gerszten, R. E.; Jaffer, F. A.; Weissleder, R. *ChemBioChem* **2002**, *3*, 207–11.
(10) Jaffer, F. A.; Tung, C. H.; Wykrzykowska, J. J.; Ho, N. H.; Houng, A. K.; Reed, G. L.; Weissleder, R. *Circulation* **2004**, *110*, 170–6.
(11) Kim, D. E.; Schellingerhout, D.; Jaffer, F. A.; Weissleder, R.; Tung, C. H. *J. Cereb. Blood Flow Metab.* **2005**, *25*, 226–33.
(12) Tung, C. H.; Ho, N. H.; Zeng, Q.; Tang, Y.; Jaffer, F. A.; Reed, G. L.; Weissleder, R. *ChemBioChem* **2003**, *4*, 897–9.
(13) Tung, C. H.; Quinti, L.; Jaffer, F. A.; Weissleder, R. *Mol. Pharm.* **2005**, *2*, 92–5.
(14) Pilch, J.; Brown, D. M.; Komatsu, M.; Jarvinen, T. A.; Yang, M.; Peters, D.; Hoffman, R. M.; Ruoslahti, E. *Proc. Natl. Acad. Sci. U.S.A.* **2006**, *103*, 2800–4.
(15) Caravan, P. *Chem. Soc. Rev.* **2006**, *35*, 512–23.
(16) Flacke, S.; Fischer, S.; Scott, M. J.; Fuhrhop, R. J.; Allen, J. S.; McLean, M.; Winter, P.; Sicard, G. A.; Gaffney, P. J.; Wickline, S. A.; Lanza, G. M. *Circulation* **2001**, *104*, 1280–5.
(17) Winter, P. M.; Caruthers, S. D.; Yu, X.; Song, S. K.; Chen, J.; Miller, B.; Bulte, J. W.; Robertson, J. D.; Gaffney, P. J.; Wickline, S. A.; Lanza, G. M. *Magn. Reson. Med.* **2003**, *50*, 411–6.
(18) Yu, X.; Song, S. K.; Chen, J.; Scott, M. J.; Fuhrhop, R. J.; Hall, C. S.; Gaffney, P. J.; Wickline, S. A.; Lanza, G. M. *Magn. Reson. Med.* **2000**, *44*, 867–72.
(19) Lanza, G. M.; Wallace, K. D.; Scott, M. J.; Cacheris, W. P.; Abendschein, D. R.; Christy, D. H.; Sharkey, A. M.; Miller, J. G.; Gaffney, P. J.; Wickline, S. A. *Circulation* **1996**, *94*, 3334–40.
(20) Sirol, M.; Fuster, V.; Badimon, J. J.; Fallon, J. T.; Moreno, P. R.; Toussaint, J. F.; Fayad, Z. A. *Circulation* **2005**, *112*, 1594–600.
(21) Botnar, R. M.; Buecker, A.; Wiethoff, A. J.; Parsons, E. C., Jr.; Katoh, M.; Katsimaglis, G.; Weisskoff, R. M.; Lauffer, R. B.; Graham, P. B.; Gunther, R. W.; Manning, W. J.; Spuentrup, E. *Circulation* **2004**, *110*, 1463–6.
(22) Spuentrup, E.; Buecker, A.; Katoh, M.; Wiethoff, A. J.; Parsons, E. C., Jr.; Botnar, R. M.; Weisskoff, R. M.; Graham, P. B.; Manning, W. J.; Gunther, R. W. *Circulation* **2005**, *111*, 1377–82.
(23) Spuentrup, E.; Fausten, B.; Kinzel, S.; Wiethoff, A. J.; Botnar, R. M.; Graham, P. B.; Haller, S.; Katoh, M.; Parsons, E. C., Jr.; Manning, W. J.; Busch, T.; Gunther, R. W.; Buecker, A. *Circulation* **2005**, *112*, 396–9.
(24) Stracke, C. P.; Katoh, M.; Wiethoff, A. J.; Parsons, E. C.; Spangenberg, P.; Spuntrup, E. *Stroke* **2007**, *38*, 1476–81.
(25) Spuentrup, E.; Katoh, M.; Buecker, A.; Fausten, B.; Wiethoff, A. J.; Wildberger, J. E.; Haage, P.; Parsons, E. C., Jr.; Botnar, R. M.; Graham, P. B.; Vettelschoss, M.; Gunther, R. W. *Invest. Radiol.* **2007**, *42*, 586–595.
(26) Spuentrup, E.; Katoh, M.; Wiethoff, A. J.; Parsons, E. C., Jr.; Botnar, R. M.; Mahnken, A. H.; Gunther, R. W.; Buecker, A *Am. J. Respir. Crit. Care Med.* **2005**, *172*, 494–500.
(27) Botnar, R. M.; Perez, A. S.; Witte, S.; Wiethoff, A. J.; Laredo, J.; Hamilton, J.; Quist, W.; Parsons, E. C., Jr.; Vaidya, A.; Kolodziej, A.; Barrett, J. A.; Graham, P. B.; Weisskoff, R. M.; Manning, W. J.; Johnstone, M. T. *Circulation* **2004**, *109*, 2023–9.
(28) Katoh, M.; Wiethoff, A. J.; Sparing, R.; Gunther, R. W.; Spuentrup, E. In *Proceedings of the International Society for Magnetic Resonance in Medicine*; Berlin, Germany, 2007; p 424.
(29) Vymazal, J.; Spuentrup, E.; Cardenas, G.; Stefancik, R.; Hartmann, M.; Uprichard, A. In *Proceedings of the Radiological Society of North America*; Chicago, 2006; p SSK06–07.
(30) Caravan, P.; Lauffer, R. B. In *Clinical Magnetic Resonance Imaging*, 3rd ed.; Edelman, R. R., Hesselink, J. R., Zlatkin, M. B., Crues, J. V., Eds.; Saunders: Philadelphia, 2005; Vol. 1, pp 357–75..
(31) Weissleder, R.; Mahmood, U. *Radiology* **2001**, *219*, 316–33.

Scheme 1. Synthesis of Peptide Tetraamine **9**

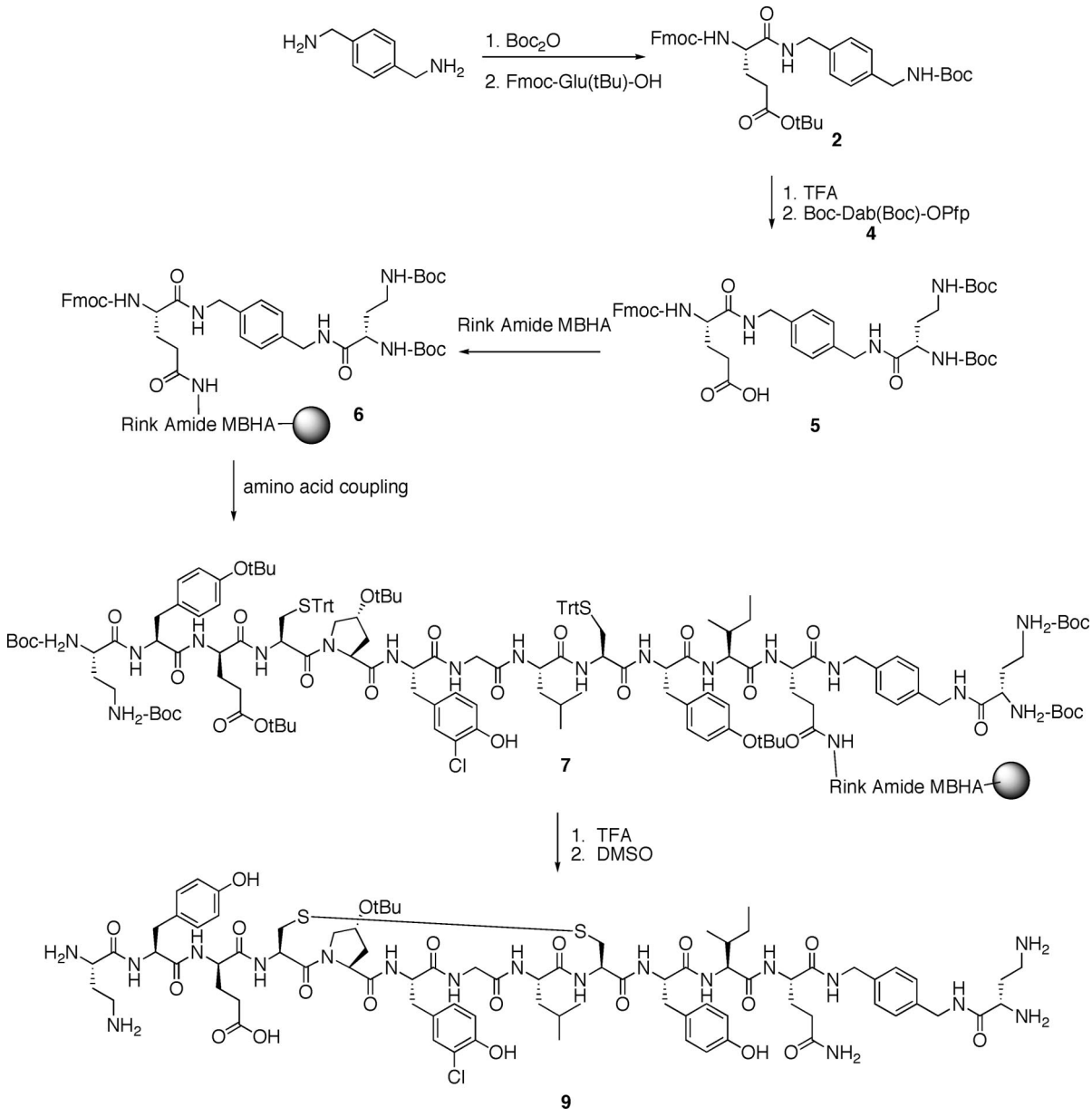

2. Results and Discussion

2.1. Synthesis of EP-2104R. The peptide portion of EP-2104R was synthesized in 18 steps (when each amino acid addition is counted) as outlined in Schemes 1 and 2. The peptide used in EP-2104R was based on a similar, all natural amino acid sequence identified using a phage display screen against human fibrin. The unnatural amino acids D-glutamate, L-3-chlorotyrosine, and hydroxyproline were found to improve fibrin binding. EP-2104R consists of an 11 amino acid peptide for targeting fibrin with 4 Gd-DOTAGA chelate moieties for MRI signal enhancement. The gadolinium chelates are linked at both the N- and C-termini. In order to facilitate coupling of the chelates to both termini, the C-terminus was first converted to an amino terminus. This was achieved by derivatizing the Rink amide MBHA resin with an amino acid−linker−amino acid moiety. Standard Fmoc-peptide chemistry was then employed to elongate the peptide on the resin. After addition of the final amino acid, the peptide was fully deprotected using an acidic cocktail (80 TFA/5 triisopropylsilane/5 1-dodecanethiol/5 dichloromethane/5 water). The peptide was cyclized in a DMSO solution. Once cyclization was complete, the peptide was purified by reversed phase chromatography.

We used the DOTAGA chelating moiety[32] to introduce gadolinium(III), Chart 1. This synthon has been used to label peptides that target the somatostatin receptor with ^{90}Y(III).[33] We chose the DOTAGA synthon for two reasons. First, the GdDOTA-like complex was expected to be highly stable and extremely inert to gadolinium loss. Second, use of this synthon results in the same donor atom set as in [Gd(DOTA)].[33] DOTA-like ligands are often conjugated to peptides using one of the carboxylates to form an amide linkage (DOTA-monoamide). However the amide oxygen donor is known to decrease the water exchange rate at the gadolinium, and this can result in decreased relaxivity.

The *tert*-butyl ester protected DOTAGA intermediate was prepared in an analogous manner to that of Eisenwiener et al.,[32] except that the stereochemistry was controlled to give the *R*-DOTAGA enantiomer.[34] The pentafluorophenyl ester was

Scheme 2. Conversion of Peptide Tetraamine **6** to EP-2104R

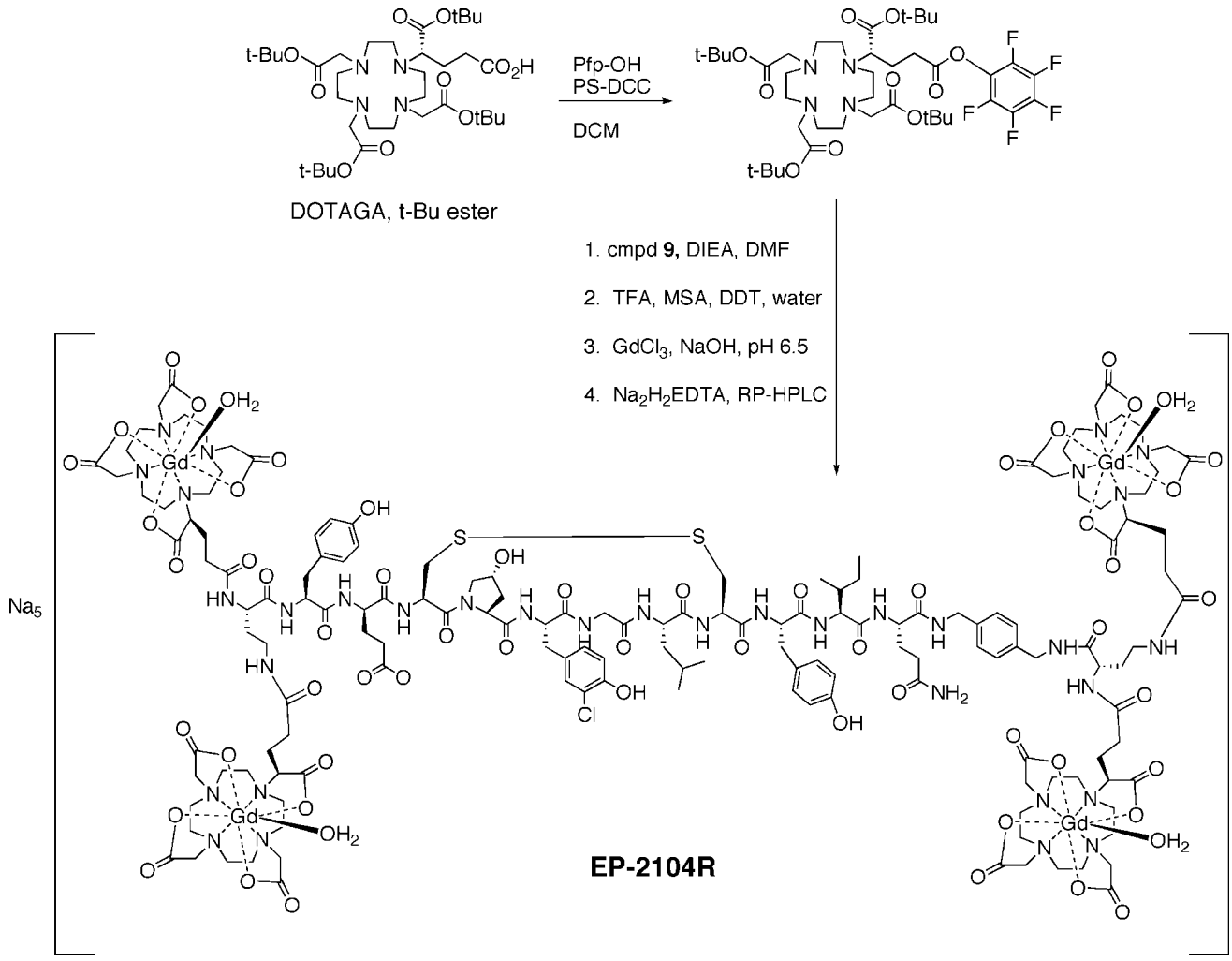

prepared, and this was used to couple to the peptide tetraamine, Scheme 2. The coupling of the four protected DOTAGA molecules to the peptide was carried out in DMF, and the reaction was monitored by HPLC. It is important to control the stoichiometry at this stage to ensure full conversion to the tetramer but at the same time minimize overacylation which results in a pentamer that is very difficult to separate from the desired product. The *tert*-butyl groups are then hydrolyzed, and the crude peptide-$(DOTAGA)_4$ ligand is chelated with $GdCl_3$ at pH 6.5. A slight excess of Gd^{3+} is used to ensure complete chelation. The excess Gd^{3+} is scavenged with EDTA, and the crude product is then purified by preparative reversed phase HPLC to give EP-2104R as the sodium salt, Scheme 2.

Direct infusion of EP-2104R for high resolution ESI-TOF MS showed a loss of the coordinated water molecules but gave the correct mass for the sodium adducts $[M + Na + H]^{2+}$ and $[M + 2Na]^{2+}$. LC-MS analysis of EP-2104R showed a single peak with the expected average mass minus the coordinated water molecules and the sodium ions which are likely dissociated during the chromatography and replaced by ammonium counterions. Thus the molecular weight seen in the LC-MS method reflects EP-2104R, minus four coordinated water molecules, and four ammonium ions. Reduction of EP-2104R with tris(2-carboxyethyl)-phosphine (TCEP) resulted in a retention time shift of 1.3 min and mass change of +2, indicating the presence of the disulfide bond (Supporting Information Figure S1). IR spectroscopy was consistent with the structure with absorptions characteristic of peptide bonds. The UV spectrum and extinction coefficients were consistent with the presence of 3 tyrosine residues and the xylene moiety. Enantiomeric purity was estimated based on chiral GC-MS,[35] and these results indicated no significant epimerization or racemization (<0.5%).

2.2. NMR Characterization of Lanthanum Analogue EP-2104R-La. Since EP-2104R is a potent NMR relaxation agent, structural characterization by NMR was impossible. Instead, the diamagnetic lanthanum(III) analogue was synthesized. EP-2104R-La shows similar LC-MS behavior to that of EP-2104R but with the expected 64 lower mass unit shift. Figure 1 shows the 1D proton NMR spectra of EP-2104R (A) and EP-2104R-La (B). While the Gd containing compound shows a broad unresolved spectrum due to enhanced relaxation, the

(32) Eisenwiener, K. P.; Powell, P.; Macke, H. R. *Bioorg. Med. Chem. Lett.* **2000**, *10*, 2133–5.
(33) Laznicek, M.; Laznickova, A.; Macke, H. R.; Eisenwiener, K.; Reubi, J. C.; Wenger, S. *Cancer Biother. Radiopharm.* **2002**, *17*, 527–33.
(34) Amedio, J., C.; Caravan, P.; Jacques, V.; Zhou, K. L.; Levy, S.; Kalageropoulos, S.; Greenfield, M. Patent Application: WO 2005/001415, 2005.
(35) Ermer, J.; Gerhardt, J.; Siewert, M. *Arch. Pharm. (Weinheim, Ger)* **1995**, *328*, 635–639.

Chart 1. Compounds Discussed in This Article

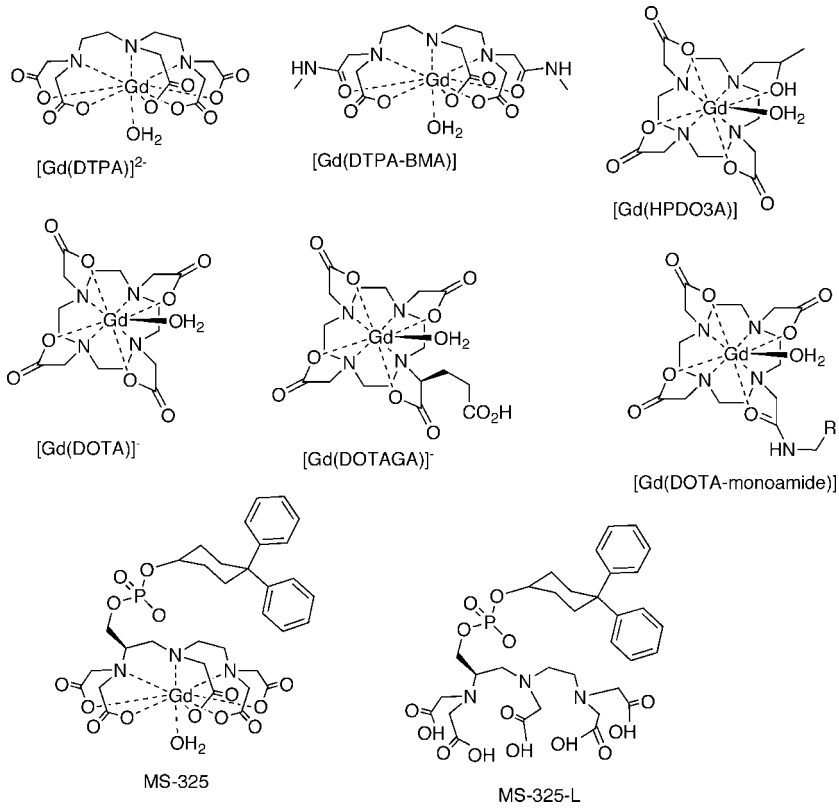

diamagnetic La analogue yields a well resolved spectrum amenable to further characterization by 2D NMR spectroscopy. Assignment of the proton resonances was obtained from 2D $^1H-^1H$ correlation spectra measured at a 400 MHz proton frequency and are listed in Supporting Information Table S2.

Figure 2 shows the H_N region of the COSY (A) and TOCSY (B) spectra obtained in H_2O/D_2O (5:1) phosphate buffer solution.[36] The individual amino acids comprising the peptide part of EP-2104R-La are readily identified by their characteristic spin coupling pattern observed in COSY and TOCSY spectra.[37] The *p*-xylenediamine (PXD) moiety and the two linker molecules, 2-diaminobutyric acid (DAB), could also be identified by their H_N-side chain couplings. Only the metal chelating DOTAGA (DTG) moieties could not be site specifically assigned due to spectral overlap. Carbon atoms directly bound to protons were assigned on the basis of 2D $^1H-^{13}C$ HSQC experiments (Table S1). The nomenclature used for the assignment is outlined in Figure 1C.

Through space contacts between protons of adjacent amino acids were observed in 2D $^1H-^1H$ NOESY spectra measured at various mixing times between 80 and 300 ms. Figure 2C shows the NOESY spectrum at the 300 ms mixing time. Sequential neighboring amino acids are identified from observation of sequential NOE connectivities within H_N-H_N, $H_N-H_{\alpha,\beta,\gamma}$, or possibly side chain−side chain correlations.[37] Along those lines, more than 110 sequential inter-residue contacts were identified which confirm the proposed sequence of EP-2104R-La as that shown in Figure 1. In addition, the presence of various NOE cross peaks between the two cysteine residues further corroborates the cyclic nature of the peptide.

The observation of long-range NOE peaks is only possible for systems with a well-defined tertiary structure. The presence of a large number of long-range connectivities (Figure 2C) therefore indicates that EP-2104R-La exhibits only one dominant conformation in solution. This enables further evaluation by NMR and molecular modeling revealing the 3D structure of the peptide in solution which will be reported elsewhere.

2.3. Kinetic Inertness and Thermodynamic Stability. For MRI contrast agents to be used clinically, it is imperative that the gadolinium remains chelated and be completely eliminated from the body. Dissociated gadolinium has been linked to a condition known as nephrogenic systemic fibrosis[38] (NSF), and this has recently prompted the U.S. Food and Drug Administration to issue a public health advisory regarding gadolinium-containing contrast agents and a possible link to the development of NSF. While it is necessary to employ a chelate with high thermodynamic stability, kinetic inertness is probably more important. For this reason the substituted DOTA chelator termed DOTAGA was used. In this way EP-2104R is an improvement over an earlier analogue, EP-1873,[27] which contains the more labile DTPA chelator (*vide infra*). The $[Gd(DOTA)]^-$ complex has a very large formation constant[39] ($\log K_{ML} = 25.3$) and is quite inert to gadolinium loss[40] or transmetalation.[41,42] It was expected

(36) Cavanagh, J.; Fairbrother, W. J.; Palmer, A. G.; Skelton, N. J. *Protein NMR Spectroscopy: Principles and Practice*; Academic Press: San Diego, 1996.
(37) Wüthrich, K. *NMR of Proteins and Nucleic Acids*; John Wiley & Sons: New York, 1986.
(38) Grobner, T.; Prischl, C. *Kidney Int.* **2007**, *72*, 260–264.
(39) Kumar, K.; Chang, C. A.; Francesconi, L. C.; Dischino, D. D.; Malley, M. F.; Gougoutas, J. Z.; Tweedle, M. F. *Inorg. Chem.* **1994**, *33*, 3567–75.
(40) Pulukkody, K. P.; Norman, T. J.; Parker, D.; Royle, L.; Broan, C. J. *J. Chem. Soc., Perkin Trans. 2* **1993**, *605*, 20.
(41) Laurent, S.; Elst, L. V.; Muller, R. N. *Contrast Media Mol. Imaging* **2006**, *1*, 128–37.

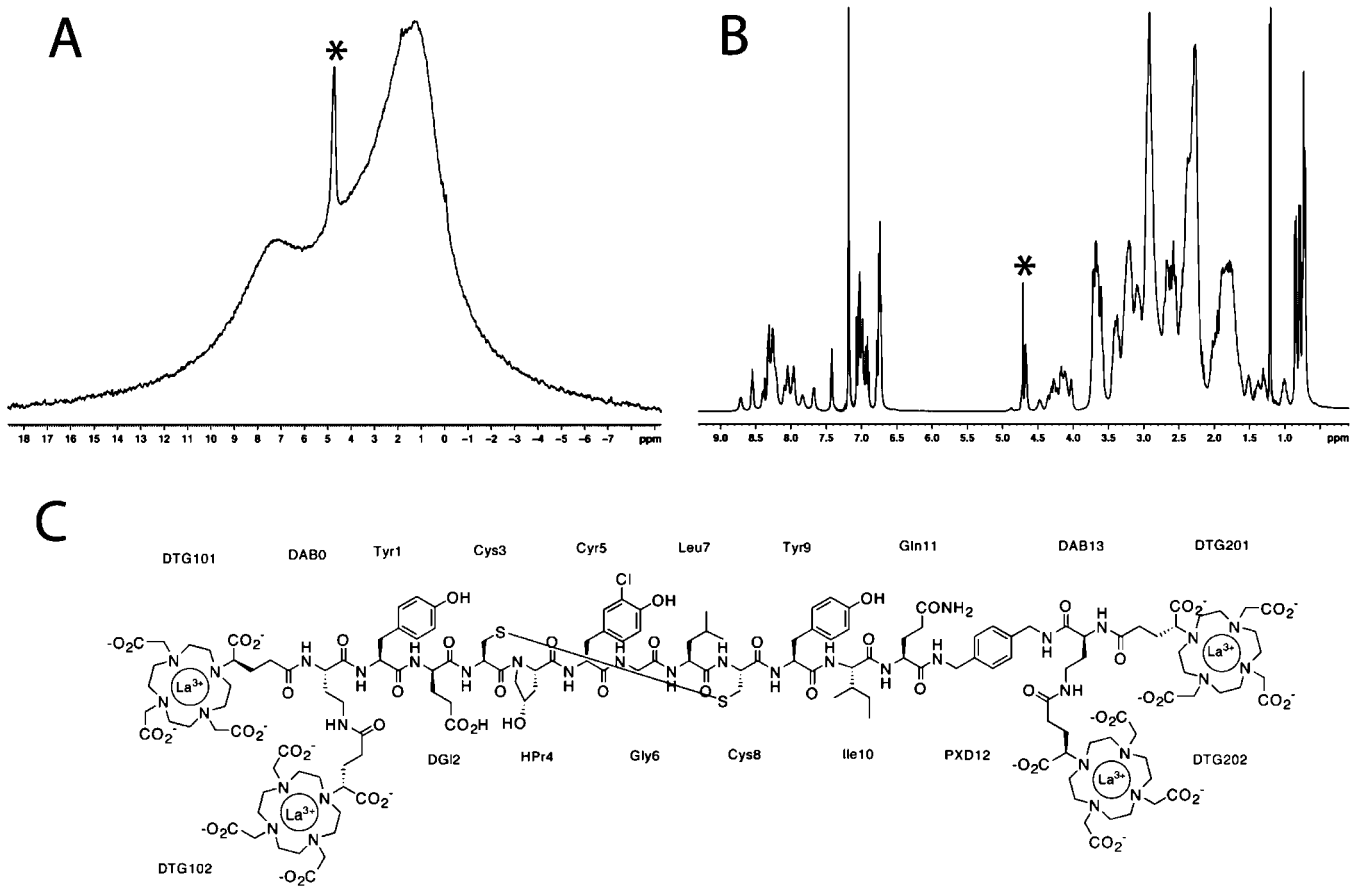

Figure 1. (A) Proton NMR spectrum of EP-2104R (ca. 2 mM in D_2O) and (B) EP-2104R-La (ca. 12 mM in H_2O/D_2O (5:1)) at 400 MHz and 300 K. Both spectra have been measured using presaturation for water suppression. The "∗" denotes the residual water signals. The nomenclature and numbering scheme used for the assignment are shown in (C).

that EP-2104R would have a similar stability and inertness with respect to Gd loss.

The presence of the peptide obviates the ability to measure thermodynamic stability and kinetic inertness as in other reports. To determine the stability constant, one needs to know the protonation constants of the ligand. However, the peptide is unstable at the high pH required to measure the protonation constants of the macrocyclic amine nitrogens. For inertness, some investigators measured gadolinium dissociation in strongly acidic media.[40] Again, at this extreme pH, the peptide is unstable to degradation. In order to get a measure of the relative stability and inertness of EP-2104R, we instead subjected EP-2104R to a challenge with a substituted DTPA ligand and compared the results to those obtained with some commercial MRI contrast agents. The ligand of MS-325 (Chart 1, denoted here as MS-325-L) was used as a challenge. This molecule has a high affinity[43] for Gd (log $K_{ML} = 22.06$), and the biphenylcyclohexyl moiety is a useful chromophore and provides retention on a reversed phase HPLC column. Transmetalation was measured by using HPLC to monitor the conversion of MS-325-L to MS-325 over time. Both MS-325 and MS-325-L were found to be stable with respect to degradation over all the pH/temperature combinations employed.

EP-2104R was extremely resistant to transmetalation. The most forcing conditions identified that did not degrade the compound were pH 3 at 60 °C for 4 days in a citric acid buffer. EP-2104R was challenged with 4 equiv of MS-325-L (1:1 in metal binder) at pH 3, pH 4, and pH 5. Figure 3 shows that transmetalation is acid catalyzed; however very little Gd is lost from EP-2104R. After 4 days, 9.6% of Gd is removed at pH 3, 1.7%, at pH 4, and 0.27%, at pH 5. It is clear from Figure 3 that the system has not equilibrated after 4 days at 60 °C. If one assumes that the protonation constants and stability constant for the EP-2104R system are the same for $[Gd(DOTA)]^-$, then one predicts that 60% of the Gd should be in the form of MS-325 at pH 3 at equilibrium.

Similar studies were performed with the macrocyclic complex [Gd(HP-DO3A)] (Prohance) and the acyclic complexes $[Gd(DTPA)]^{2-}$ (Magnevist) and [Gd(DTPA-BMA)] (Omniscan) at pH 3 and pH 5 at 60 °C. The structures of these commercial agents are shown in Chart 1. For the acyclic ligands, the transmetalation reaction was complete within 10 min at both pH values. The equilibrium result was very close to that predicted based on reported stability constants measured at 25 °C. For example at pH 5, $[Gd(DTPA)]^{2-}$ lost 71.7% of its Gd compared to the 71.1% predicted,[43,44] and [Gd(DTPA-BMA)] lost 88.4% of its Gd compared to the 86.6% predicted.[43,45] The macrocyclic complex [Gd(HP-DO3A)] was more inert. Figure

(42) Laurent, S.; Elst, L. V.; Copoix, F.; Muller, R. N. *Invest. Radiol.* **2001**, *36*, 115–22.
(43) Caravan, P.; Comuzzi, C.; Crooks, W.; McMurry, T. J.; Choppin, G. R.; Woulfe, S. R. *Inorg. Chem.* **2001**, *40*, 2170–6.
(44) Martell, A. E.; Smith, R. M.; Motekaitis, R. J. *NIST Critically Selected Stability Constants of Metal Complexes: NIST Standard Reference Data 46*, 3.0 ed.; National Institute of Standards and Technology: Washington, DC, 1997.
(45) Cacheris, W. P.; Quay, S. C.; Rocklage, S. M. *Magn. Reson. Imaging* **1990**, *8*, 467–81.

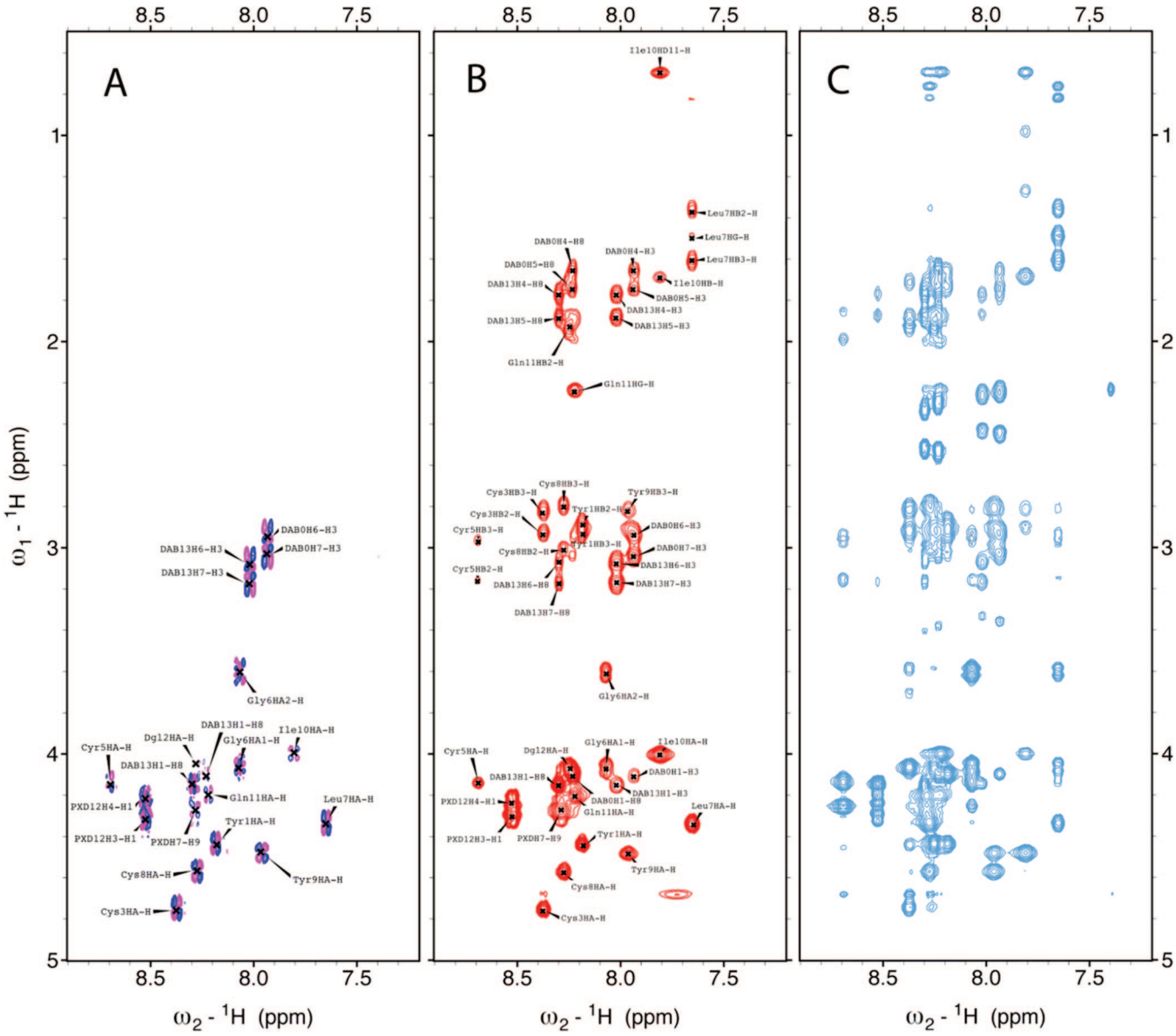

Figure 2. Amide proton region of the 2D $^1H-^1H$ correlation spectra of EP-2104R-La (ca. 12 mM) at 400 MHz and 300 K in H_2O/D_2O (5:1) buffer. (A) Double-quantum filtered COSY spectrum, (B) TOCSY spectrum with 80 ms MLEV-17 spin lock, (C) NOESY spectrum at 300 ms mixing time. All spectra are acquired with a watergate pulse sequence for water suppression.[36] The assignments in (C) have been omitted for clarity.

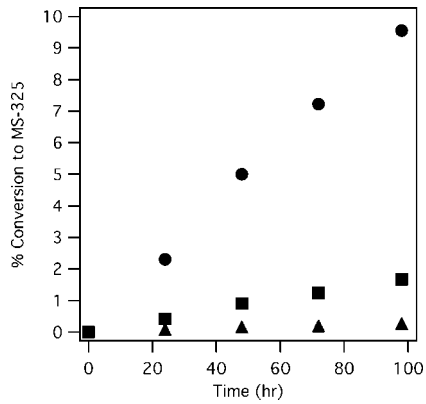

Figure 3. Time course of reaction of EP-2104R with 4 equiv MS-325-L (1:1 in chelator) showing conversion to product MS-325 at 60 °C in citrate buffer at pH 3 (●), pH 4 (■), or pH 5 (▲).

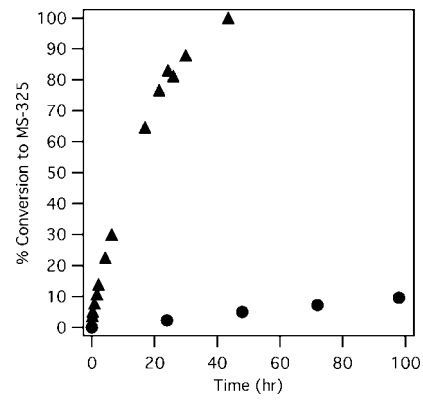

Figure 4. Time course of reaction of MS-325-L with either EP-2104R (●) or [Gd(HP-DO3A)] (▲) and conversion to MS-325 at pH 3, citrate buffer, 60 °C.

4 shows gadolinium loss as a function of time for [Gd(HP-DO3A)] and EP-2104R at pH 3. The [Gd(HP-DO3A)] system has reached equilibrium by 44 h (99.8% Gd loss compared to 96.2% predicted[39,43]). At pH 5, [Gd(HP-DO3A)] is more inert and has not reached equilibrium at 48 h (39.2% loss vs 92.6% predicted).

These studies demonstrate that EP-2104R is much more inert to gadolinium transmetalation than commercially available contrast agents. Figure 4 shows that EP-2104R is significantly more inert than [Gd(HP-DO3A)], which itself has been shown to be very robust with respect to gadolinium loss under a number of challenges.[41,42,46] Under physiological conditions where the temperature is lower (37 °C), pH is higher (7.4), and endogenous chelators are less potent than MS-325-L, it is highly unlikely that EP-2104R will release gadolinium in vivo.

2.4. Binding of EP-2104R to Human Fibrin. Fibrin binding localizes EP-2104R to the site of clotting and thus is critical to the EP-2104R mechanism of action. Fibrin is an insoluble polymer formed during the clotting cascade by thrombin-induced polymerization of a soluble fibrinogen monomer, followed by Factor XIII mediated cross-linking. In these *in vitro* studies, fibrin is generated by adding thrombin and calcium to fibrinogen and allowing the solution to polymerize to a gel state. Here, fibrin concentrations refer to that of the polymerized monomeric fibrinogen unit.

Binding of EP-2104R to human fibrin in plasma was measured by equilibrium binding at 37 °C in two assay formats: with a plasma-derived clot or with purified fibrin. In the plasma clot assay, known concentrations of EP-2104R were incubated in human plasma, and thrombin was added to induce clot formation. The clot was separated from the serum, and the concentration of EP-2104R in the serum ($[EP\text{-}2104R]_{free}$) was determined by ICP-MS analysis; the concentration of fibrin-bound EP-2104R in the clot was calculated by subtraction ($[EP\text{-}2104R]_{bound} = [EP\text{-}2104R]_{total} - [EP\text{-}2104R]_{free}$). The plasma used contained a functional fibrinogen concentration of 2.3 mg/mL, within the range of normal plasma, 2.0–3.0 mg/mL.[47] This value was used to calculate the moles of EP-2104R bound per mole of fibrin for each data point.

In the second assay, purified fibrinogen (2.5 mg/mL; 7 μM fibrin) was clotted with thrombin and dried to a thin film in wells of a microtiter plate. The resulting clots bind to the plate without loss of protein. The fibrin is condensed into a thin disk that is rapidly penetrated by EP-2104R and other molecules of similar molecular weight (full equilibration occurs within 30 min) and is without the diffusion limitations posed by other binding assays. The clots were rehydrated with plasma containing known concentrations of EP-2104R dissolved in human citrated plasma. After incubation at 37 °C, the concentration of EP-2104R in the supernatant ($[EP\text{-}2104R]_{free}$) was determined by ICP-MS. The contents of the media or the fibrin structure can be further modified to test the effects of specific proteins, buffer conditions, or fibrin organization on fibrin binding. Dried fibrin prepared by this procedure is comparable in structure to freshly polymerized fibrin. SDS-PAGE of fibrin prepared by this procedure indicated that the fibrin is fully cross-linked by factor XIII at the γ subunits. Studies from other laboratories have shown that the dried and rehydrated fibrils bear a similar morphology to freshly polymerized fibrin when examined by electron microscopy and that fibrin specific antibodies, but not fibrinogen specific antibodies, react with dried fibrin.[48]

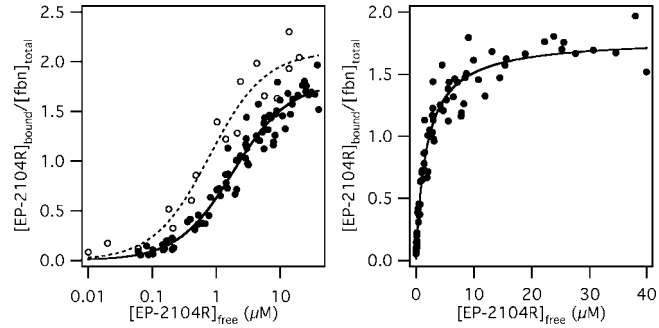

Figure 5. (Left) EP-2104R binding to human fibrin in the presence of human plasma in two assay formats: a plasma derived clot (open circles) and a plate-based assay using purified fibrin (filled symbols). Lines are fits to the data as described in the text. (Right) Data from plate assay plotted on a linear scale to highlight saturation of binding sites at ~2 sites per fibrin monomer.

Table 1. Comparison of EP-2104R Binding to Different Animal Fibrins Measured Either in the Species' Plasma, in TBS, or in 4.5% HSA[a]

fibrin source	medium	K_d (μM)	N binding sites
human	TBS	1.7 ± 0.5	2.2 ± 0.1
human	4.5% HSA in TBS	1.7 ± 0.5	2.2 ± 0.2
human	human plasma	1.6 ± 0.2	1.7 ± 0.4
pig	pig plasma	4.9 ± 0.9	1.7 ± 0.1
dog	dog plasma	2.2 ± 0.3	1.6 ± 0.05
rabbit	rabbit plasma	2.4 ± 0.3	2.0 ± 0.1
rat	rat plasma	1.8 ± 0.1	1.7 ± 0.1
mouse	mouse plasma	1.5 ± 0.3	1.7 ± 0.1

[a] Relaxivity has units of $mM^{-1}\ s^{-1}$. Binding parameters derived from best-fits to data ($[EP\text{-}2104R]_{bound}$ vs $[EP\text{-}2104R]_{free}$) using eq 1.

For both assays, the data were fit to a model of N equivalent binding sites with the dissociation constant, K_d, with units of μM, given by eq 1:[51]

$$\frac{[EP\text{-}2104R]_{bound}}{[fbn]_{total}} = \frac{N \times [EP\text{-}2104R]_{free}}{([EP\text{-}2104R]_{free} + K_d)} \qquad (1)$$

where the total fibrin (fbn) concentration is the concentration of polymerized fibrinogen monomer in μM. The data with fitted curves are shown in Figure 5. These two different methods (plasma clot vs dried fibrin assay) yield comparable results, in both the estimated number of binding sites (1.9 ± 0.1 vs 1.7 ± 0.1) and the K_d (0.9 ± 0.3 vs 1.6 ± 0.2), respectively.

Figure 5 shows binding of EP-2104R in the presence of human plasma. The fibrin plate assay was also run with EP-2104R in buffer or EP-2104R in 4.5% HSA solution, and very similar dissociation constants were obtained, Table 1. The congruence of results obtained in the presence and absence of plasma proteins indicates that EP-2104R has a high degree of binding specificity for fibrin over proteins in plasma, particularly serum albumin. This property is especially important, as binding to plasma proteins would reduce binding to the target, increase background MRI enhancement by the agent, and slow clearance of nonclot associated compounds from the vasculature (which also contributes to signal background).

The ~15% difference between an exact 2.0 sites per fibrin monomer and the observed data in the fibrin plate assay may

(46) Kumar, K.; Chang, C. A.; Tweedle, M. F. *Inorg. Chem.* **1993**, *32*, 587–93.
(47) Redman, C. M.; Xia, H. *Ann. N.Y. Acad. Sci.* **2000**, *936*, 480–95.
(48) Tymkewycz, P. M.; Creighton-Kempsford, L. J.; Hockley, D.; Gaffney, P. J. *Thromb. Haemost.* **1992**, *68*, 48–53.

Table 2. Relaxivities for EP-2104R in Various Media Measured at 0 < [EP-2104R] < 40 μM, 37 °C, pH 7.4 and Expressed on a per Gadolinium and per Molecule Basis[a]

	r_1 (20 MHz)		r_1 (60 MHz)		r_2 (60 MHz)	
medium	per Gd	per molecule	per Gd	per molecule	per Gd	per molecule
TBS	11.1 (0.7)	44.4 (2.8)	10.1 (0.1)	40.3 (0.3)	12.8 (0.2)	51.1 (0.6)
Fgn/TBS	12.4 (0.8)	49.4 (3.2)	11.1 (0.7)	44.2 (2.9)	14.4 (0.9)	57.4 (3.7)
Fgn/plasma	11.2 (0.7)	44.8 (2.9)	10.6 (0.7)	42.2 (2.7)	12.4 (0.8)	49.6 (3.2)
fbn/TBS	24.8 (0.7)	99.3 (2.8)	17.9 (0.3)	71.4 (1.2)	32.1 (2.1)	128.2 (8.3)
clotted plasma	24.9 (1.6)	99.7 (6.5)	17.8 (1.2)	71.2 (4.6)	27.7 (1.8)	110.7 (7.2)
$[Gd(DOTA)]^-$	3.4	3.4	2.9[b]	2.9[b]	3.2[b]	3.2[b]

[a] Relaxivity has units of mM^{-1} s^{-1}. The number in parentheses corresponds to one standard deviation. Relaxivities for $[Gd(DOTA)]^-$ in water at 37 °C are provided for reference.[56] [b] measured at 64 MHz.

be attributed to several sources. There is some uncertainty as to the functional protein concentration. An extinction coefficient determined from the literature for pure fibrin monomer was used which may not correspond exactly to the commercial preparations used in this study. Reduction in site accessibility may have occurred at the protein−plate interface. A small percentage of the fibrin molecule in the preparation may also be misfolded and not competent to bind. Nonetheless, the availability of two sites per fibrin monomer is consistent with the 2-fold symmetry of the fibrinogen molecule, an $\alpha_2\beta_2\gamma_2$ oligomer of three protein chains. The ability to bind to two sites on each fibrin molecule effectively doubles the potential concentration of EP-2104R that may localize in a clot, greatly enhancing the signal that may be obtained with this agent.

In order to address the question of whether the binding sites were equivalent and independent, the data were also fit to a more general stoichiometric model of binding[49,50] where the binding sites are not assumed to be equivalent. This fit returned binding constants that were statistically equivalent indicating that there is no cooperativity in the binding of EP-2104R binding to fibrin and that the two sites do in fact behave independently.[51]

The fibrin concentration in thrombi is expected to be rather high since the circulating fibrinogen concentration is ~7 μM. During the clotting process, the fibrin concentration at the clot increases further by ongoing fibrin formation as well as clot retraction, resulting in 10s to 100s μM fibrin. The low micromolar affinity of EP-2104R coupled with the high micromolar concentration of binding sites in thrombi assures appreciable binding of EP-2104R to clots as has been reported in various animal models.

The peptide portion of EP-2104R (without the 4 gadolinium chelates) was also assessed for fibrin affinity. The affinity of EP-2104R was 2.5 times lower than that of the parent peptide. This reduction in affinity may be expected given the bulk of the 4 GdDOTAGA moieties (~75% of the total EP-2104R molecular weight). However the affinity loss is not dramatic suggesting that C- and N-terminal substitution is well tolerated.

2.5. Species Dependence on Fibrin Binding. The dried fibrin assay was also utilized to determine the affinity of EP-2104R for fibrin from other species. In a similar manner, purified fibrinogen from pig, dog, rabbit, rat, or mouse plasma was used to create fibrin plates. The binding of EP-2104R to these fibrins was then assessed in the presence of that species' blood plasma. The data are reported in Table 1. There was no strong species dependence on affinity. All species showed low micromolar affinity to two equivalent binding sites, indicating that critical residues in the EP-2104R binding site are largely conserved between species.

2.6. Relaxivity of EP-2104R in Different Media. The efficiency of contrast agents in terms of their ability to enhance the solvent–water relaxation rate is defined as relaxivity, r_1, which is the degree to which a given concentration can change $1/T_1$:

$$r_1 = \frac{\Delta(1/T_1)}{[\mathrm{Gd}]} \tag{2}$$

A higher relaxivity will enable detection of the agent at lower concentrations. Relaxivity is dependent on the applied magnetic field and on many molecular parameters. Because of this, relaxivity measurements were carried out at several field strengths in different media. The proton relaxivity of EP-2104R was measured at 20 and 60 MHz in Tris buffered saline (TBS), in the presence of fibrinogen, in a fibrin gel, in human plasma, and in clotted human plasma at 37 °C. The results are summarized in Table 2. Data were collected at 20 MHz because there is a large body of relaxivity data at 20 MHz with which to compare. However 60 MHz is closer to the common clinical imaging frequency of 64 MHz (1.5 T) used on the majority of clinical imagers. The data in Table 2 are reported on a per gadolinium basis to better compare with other compounds and on a per molecule basis to better relate T_1 change associated with fibrin binding.

The per Gd relaxivity in TBS is about 3-fold higher for EP-2104R than for $[Gd(DOTA)]^-$. This is attributed to the larger size of EP-2104R which results in a longer rotational correlation time. Increasing the correlation time is an established method to increase relaxivity.[15,52,53] The correlation time can also be increased by protein binding. Lauffer[54] proposed noncovalent binding of contrast agents to target proteins as a means of increasing relaxivity many years ago, and this strategy was successfully employed with MS-325 targeting serum albumin[49,55] and with numerous compounds since. In the case of fibrin binding, the relaxivity of EP-2104R more than doubles at 20 MHz and sees an 80% increase at 60 MHz. The relaxivity is similar when measured in either fibrin gel or in a plasma clot.

(49) Caravan, P.; Cloutier, N. J.; Greenfield, M. T.; McDermid, S. A.; Dunham, S. U.; Bulte, J. W.; Amedio, J. C., Jr.; Looby, R. J.; Supkowski, R. M.; Horrocks, W. D., Jr.; McMurry, T. J.; Lauffer, R. B. *J. Am. Chem. Soc.* **2002**, *124*, 3152–62.
(50) Klotz, I. M. *Ligand Receptor Energetics - A Guide for the Perplexed*; John Wiley & Sons: New York, 1987.
(51) Koshland, D. E., Jr.; Nemethy, G.; Filmer, D. *Biochemistry* **1966**, *5*, 365–85.
(56) Rohrer, M.; Bauer, H.; Mintorovitch, J.; Requardt, M.; Weinmann, H. J. *Invest. Radiol.* **2005**, *40*, 715–24.
(52) Caravan, P.; Ellison, J. J.; McMurry, T. J.; Lauffer, R. B. *Chem. Rev.* **1999**, *99*, 2293–352.
(53) Lauffer, R. B. *Chem. Rev.* **1987**, *87*, 901–927.
(54) Lauffer, R. B. *Magn. Reson. Med.* **1991**, *22*, 339.
(55) Lauffer, R. B.; Parmelee, D. J.; Dunham, S. U.; Ouellet, H. S.; Dolan, R. P.; Witte, S.; McMurry, T. J.; Walovitch, R. C. *Radiology* **1998**, *207*, 529–538.

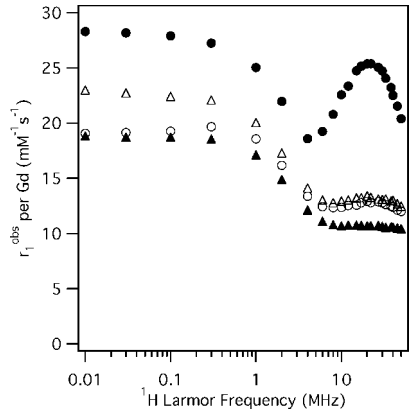

Figure 6. Nuclear magnetic relaxation dispersions (NMRD) displayed as observed relaxivity per gadolinium of 50 μM EP-2104R in Tris buffered saline (▲), human blood plasma (△), 30 μM fibrinogen solution (○), or 30 μM gelled fibrin (●) at 35 °C.

On the other hand, if relaxivity is measured in fibrinogen solution or in unclotted plasma, the values are closer to those obtained in buffer.

At 60 MHz, the relaxivity of EP-2104R in fibrin is about 6 times higher than that of[Gd(DOTA)] on a per gadolinium basis and 25 times higher on a per molecule basis. It is this increased sensitivity that allows for robust detection of thrombi in a variety of in vivo models.

To gain a better understanding of the field dependence on relaxivity, nuclear magnetic relaxation dispersion (NMRD) profiles were measured at 35 °C. Here relaxation rates are recorded at different frequencies for TBS, fibrinogen solution, fibrin gel, or human plasma in the presence or absence of EP-2104R, and relaxivity at each frequency in each medium is calculated according to eq 22. The profiles are shown in Figure 6. The NMRD profile of EP-2104R in fibrin gel is typical of a protein bound gadolinium complex. The increasing relaxivity between 4 and 30 MHz followed by dispersion is indicative of a slow motion component inducing relaxation, i.e., a slow motion arising from docking to the protein.[15] Solomon−Bloembergen−Morgan [52,57–59] theory predicts that as the correlation time gets longer, the relaxivity should increase in this high frequency region. The curve should be rather flat at short correlation times and then take on this peaked appearance in this 4–60 MHz frequency range as the correlation time gets longer.[15] In principle these profiles can be modeled. However given the structural complexity of EP-2104R it is obvious that rotational motion cannot be attributed to a single isotropic correlation time. Moreover it is not clear whether the correlation time for each gadolinium center would be the same. This leads to too many assumptions and more parameters than can be meaningfully fit.

For the fibrinogen and plasma solutions, relaxivity is enhanced slightly at all frequencies. There is also a hint of this peaked effect at higher frequencies suggesting that there may be a small fraction of the compound bound to fibrinogen or plasma proteins.

To verify that the relaxivity increase in the fibrin gel was not due to some microviscosity effect, the relaxivity of [Gd(DTPA)]$^{2-}$ was also measured in fibrin gel. The relaxivity of [Gd(DTPA)]$^{-}$ was unaffected by the presence of the 1% fibrin gel, suggesting that the increased relaxivity observed is due to fibrin binding.

2.7. Specificity of EP-2104R for Fibrin. For effective imaging of thrombi, which by definition reside in blood vessels, it is important that the imaging agent displays specificity for fibrin over blood plasma proteins. Of particular concern is fibrinogen (Fgn) which obviously shares a great deal of structural homology with fibrin and is present at a circulating concentration of ~7.5 μM. The peptide portion of EP-2104R is based on a sequence identified by phage display against fibrin,[60] and in that selection the phage library was first prescreened against fibrinogen to exclude fibrinogen binders. The NMRD data shown in Figure 6 suggests that there is not a large fraction of EP-2104R bound to fibrinogen, otherwise one would have expected the relaxivity to be enhanced as in the fibrin gel.

The binding of EP-2104R to fibrinogen was assessed with two techniques. We used isothermal titration calorimetry to measure the heat change that occurs when a ligand binds to a protein target. No significant heat change was detected for the titration of 20 mM EP-2104R with 59.7 μM Fgn, indicating that the interaction between EP-2104R and fibronogen is weak. From the calorimetry studies, a lower limit of a dissociation constant could be estimated, $K_d > 100$ μM for the binding of EP-2104R to fibrinogen.

The proton relaxation enhancement (PRE) effect was also used to estimate EP-2104R binding to Fgn. In the case of EP-2104R binding to a single site on fibrinogen, there should be two species in solution: free (unbound) and fibrinogen bound. These are related by a dissociation constant, K_d, eq 3.

$$K_d = \frac{[\text{EP-2104R}]_f([\text{Fgn}]_{tot} - [\text{EP-2104R}]_b)}{[\text{EP-2104R}]_b} \quad (3)$$

Here, $[\text{EP-2104R}]_f$ refers to the concentration of free (unbound) EP-2104R, and the bound concentration is denoted $[\text{EP-2104R}]_b$. The total fibrinogen concentration is denoted $[\text{Fgn}]_{tot}$. The bound and free EP-2104R will have different relaxivies, r_{1f} and r_{1b} respectively, and the measured relaxation rate ($1/T_1$) will depend on these relaxivities and the concentrations of the two species, eq 44.

$$\frac{1}{T_1} = r_{1f}[\text{EP-2104R}]_f + r_{1b}[\text{EP-2104R}]_b + \frac{1}{T_1^0} \quad (4)$$

Here, $1/T_1{}^0$ is the relaxation rate of the solution in the absence of EP-2104R. Alternately one can rearrange eq 4 to calculate the observed relaxivity as defined by eq 5.

$$r_1^{obs} = \frac{\frac{1}{T_1} - \frac{1}{T_1^0}}{[\text{EP-2104R}]_{tot}} = f_f r_{1f} + f_b r_{1b} \quad (5)$$

Here f refers to the fraction of EP-2104R that is either free (f_f) or bound to fibrinogen (f_b). The concentration of EP-2104R bound can be calculated from the initial concentrations (totals) of EP-2104R and fibrinogen if the K_d is known, eq 6:

$$[\text{EP-2104}]_b = \frac{a - \sqrt{a^2 - 4[\text{Fgn}]_t[\text{EP-2104}]_t}}{2}; \quad a = [\text{Fgn}]_t + [\text{EP-2104}]_t + K_d \quad (6)$$

(57) Bloembergen, N. *J. Chem. Phys.* **1957**, *27*, 572–573.
(58) Bloembergen, N.; Morgan, L. O. *J. Chem. Phys.* **1961**, *34*, 842–850.
(59) Solomon, I. *Phys. Rev.* **1955**, *99*, 559.
(60) Wescott, C. R.; Nair, S. A.; Kolodziej, A.; Beltzer, J. P. Patent Application WO2001009188, 2001.

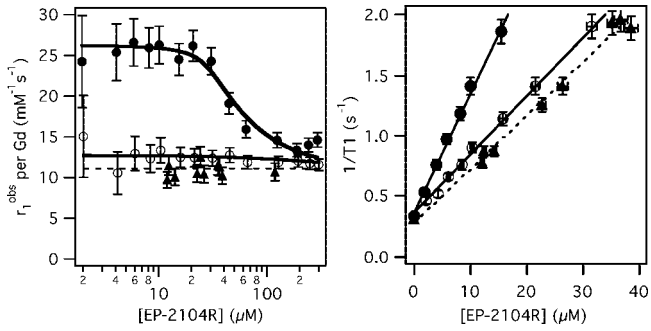

Figure 7. Effect of increasing amounts of EP-2104R on observed relaxivity in 30 μM fibrin (●), 30 μM fibrinogen (○), or buffer (▲) measured at 20 MHz (left panel). Right panel: same data, plotted as relaxation rate ($1/T_1$) at low EP-2104R concentrations to demonstrate the small but significant relaxation enhancement due to weak fibrinogen binding. Solid lines are fits to the data as described in the text.

The relaxivity of the unbound fraction is known from measurements in the absence of protein, Table 2. It is assumed that the relaxivity of the fibrinogen-bound fraction is the same as the relaxivity for EP-2104R bound to fibrin, Table 2. One can iteratively vary K_d until the calculated and observed relaxation rates or relaxivities agree. In principle, the relaxivity of fibrinogen-bound EP-2104R can also be obtained from fitting the data; however for weak binding K_d and r_{1b} are correlated, so we make the reasonable assumption that r_{1b} is the same for fibrinogen and fibrin binding.

A series of solutions of EP-2104R (0–300 μM) were prepared at a fixed 30 μM fibrinogen concentration. T_1 was measured at both 20 and 60 MHz before and after polymerizing the fibrinogen to fibrin via addition of thrombin and Ca^{2+}. The left panel of Figure 7 shows the results of the experiments at 20 MHz plotted as observed relaxivity (r_1^{obs}) versus total EP-2104R concentration, along with measurements made in the absence of protein. The solid line through the fibrin relaxivity data in Figure 7 is calculated based on the binding data in Table 1. The relaxivity data are in accord with the equilibrium binding studies. Note that after the two fibrin binding sites are saturated, the relaxivity decreases and begins to approach r_{1f} at very high concentrations.

There is a small but significant increase in r_1^{obs} for EP-2104R in fibrinogen relative to buffer-only. In the left panel of Figure 7, the uncertainties in each individual relaxivity data point are large because at low EP-2104R concentrations the difference between $1/T_1$ and $1/T_1^0$ is small compared to the uncertainty in T_1 (5%). This is compounded by dividing this difference by the small EP-2104R concentration (estimated at ±3%) to obtain r_1^{obs}. However the measured $1/T_1$ data are more compelling and are shown in the right panel of Figure 7 with the same error bars (±5% in T_1, ±3% in concn). The fibrinogen $1/T_1$ data consistently lie above the dashed line denoting the slope (relaxivity) of the $1/T_1$ data in the absence of protein. Fitting the fibrinogen data (solid line) as described above resulted in $K_d = 240 \pm 30$ μM for EP-2104R binding to fibrinogen. EP-2104R displays a 100-fold higher selectivity for fibrin than for fibrinogen. Although there are two sites on fibrin for EP-2104R, we assumed the simplest binding model for the fibrinogen interaction (one site) since binding to fibrinogen is so weak (≤11% bound with [Fgn] at 4 times physiological levels). Protein solubility limits the degree of site occupancy that can be achieved.

The NMRD data in human plasma, Figure 6, were not consistent with strong binding to plasma proteins. To further assess plasma protein binding, the interaction of EP-2104R with the most abundant plasma protein, human serum albumin (HSA), was investigated. In the dried fibrin binding assay, there was no discernible difference in EP-2104R binding to fibrin if the assay was carried out in Tris buffered saline, in 4.5% HSA solution, or in human plasma indicating that HSA or other plasma proteins do not compete with fibrin from EP-2104R binding. Isothermal calorimetry using a 560 μM HSA solution to titrate a 20 mM EP-2104R solution showed no significant heat changes indicating weak protein binding. Using the PRE method and a 670 μM HSA solution, a K_d of 4600 ± 460 μM was estimated for the binding of EP-2104R to serum albumin, over a 1000-fold lower affinity than that for binding to fibrin.

3. Conclusions

EP-2104R consists of an 11 amino acid peptide functionalized with two GdDOTAGA moieties at each of the C- and N-termini. The peptide imparts high affinity for fibrin, the most concentrated component of blood clots, and 100- to 1000-fold higher selectivity for fibrin compared to blood plasma proteins such as fibrinogen or serum albumin. The fibrin affinity and selectivity explain the localization of EP-2104R to thrombi observed in various animal models[20–26] and clinical studies.[28,29] The four GdDOTAGA moieties provide a significant relaxation enhancement effect that allows EP-2104R to enhance thrombi in MR images. The relaxivity of EP-2104R bound to fibrin at 37 °C is about 25 times higher than that of $[Gd(DOTA)]^-$ at the clinical field strength of 1.5 T. This combination of strong fibrin binding, fibrin selectivity, and high molecular relaxivity is why EP-2104R appears effective at detecting blood clots in vivo.

4. Experimental Section

4.1. Materials. Human fibrinogen, grade L (Lots 18 and 21) was purchased from American Diagnostica. Citrated human plasma (Product Code 19201) was received from Red Cross, Danvers, MA. The buffer used in these studies was 50 mM tris(hydroxymethyl)aminomethane (Tris) buffered saline (TBS). The thrombin was obtained from Haematologic Technologies, diluted 1:100 into TBS, and frozen as aliquots. These aliquots had activities of 0.3–0.4 NIH Units/μL. Calcium chloride solution (2 M) was prepared in water from reagent grade material. The commercial contrast agents were obtained as 0.5 M formulated solutions: $[Gd(DTPA)]^{2-}$ (with *N*-methylglucamine as the counterion, Magnevist, Berlex, Wayne, NJ), [Gd(HP-DO3A)] (Prohance, Bracco, Princeton, NJ), and [Gd(DTPA-BMA)] (Omniscan, GE Healthcare, Princeton, NJ). Citric acid (Sigma) and sodium citrate (JT Baker) were USP grade. The derivatized DTPA ligand for MS-325, denoted here as MS-325-L, was synthesized as described previously.[61] High resolution ESI-TOF mass spectra were recorded at Tandem Laboratories (Woburn, MA).

4.2. Synthesis of EP-2104R. 4.2.1. *tert*-Butyl 4-(aminomethyl)benzylcarbamate, 1. *p*-Xylylenediamine (75.0 g, 550.6 mmol) was dissolved in dioxane (1 L) at room temperature. Di-*tert*-butyldicarbonate (60.0 g, 275.3 mmol) was dissolved in dioxane (0.5 L) and added dropwise to the solution over 5 h at room temperature. A solid precipitated, was filtered, and washed with dioxane (200 mL). The filtrate was concentrated to a volume of 400 mL under reduced pressure. The solution was then poured into water (1400 mL). A precipitate formed, was filtered, and washed with water (200 mL). The filtrate was then extracted with ethyl acetate (4 × 500 mL). The combined extracts were dried over

(61) McMurry, T. J.; Parmelee, D. J.; Sajiki, H.; Scott, D. M.; Ouellet, H. S.; Walovitch, R. C.; Tyeklar, Z.; Dumas, S.; Bernard, P.; Nadler, S.; Midelfort, K.; Greenfield, M.; Troughton, J.; Lauffer, R. B. *J. Med. Chem.* **2002**, *45*, 3465–74.

sodium sulfate and concentrated under reduced pressure to give **1** (32.7 g, 50% yield) as a pale beige solid. ^{1}H NMR (300 MHz, DMSO-d_6): 7.28 (d, 2H, ^3J = 8 Hz), 7.18 (d, 2H, ^3J = 8 Hz), 4.09 (d, 2H, ^3J = 6 Hz), 3.75 (s, 2H), 1.38 (s, 9H). ^{13}C NMR: 156.2, 141.0, 139.0 127.6, 127.2, 78.0, 45.0, 43.5, 28.6. High resolution ESI-TOF-MS: *m*/*z* expected $[C_{13}H_{20}N_2O_2 + H]^+$ 237.1604, found 237.1392.

4.2.2. 1-Fmoc-Glu(*t*Bu)-*tert*-butyl-4-(aminomethyl)benzylcarbamate, 2. 1 (32.0 g, 135.4 mmol) was dissolved in dimethylformamide (300 mL). Fmoc-Glu(*t*Bu)-OH (54.7 g, 128.6 mmol), EDC (24.6 g, 128.6 mmol), and 1-hydroxybenzotriazole (17.4 g 128.6 mmol) were dissolved acetonitrile (1.2 L) and stirred for 15 min at room temperature. The amino acid solution was added to the amine solution, and the reaction was stirred for 2 h at room temperature. The reaction mixture was then concentrated to a volume of 300 mL under reduced pressure and poured into water (1.7 L). The resulting solid was filtered, washed with water (600 mL), and dried under reduced pressure to give **2** (96.59 g). This compound was not purified further and used crude in the next step. ^{1}H NMR (300 MHz, DMSO-d_6): 8.34 (t, 1H, ^3J = 6 Hz), 7.89 (d, 2H, ^3J = 8 Hz), 7.72 (m, 2H), 7.58–7.24 (m, 6H), 7.18 (s, 4H), 4.27 (m, 4H), 4.07 (m, 4H), 2.24 (t, 2H, ^3J = 7.5 Hz), 1.93 (m, 1H), 1.70 (m, 1H), 1.40 (s, 9H), 1.38 (s, 9H). ^{13}C NMR: 172.0, 156.7, 144.3, 141.1, 139.2, 138.2, 138.1, 128.0, 127.4, 127.3, 125.7, 120.5, 80.1, 78.1, 66.0, 54.6, 47.0, 43.5, 42.2, 31.9, 28.6, 28.2, 27.7. High resolution ESI-TOF-MS: *m*/*z* expected $[C_{37}H_{45}N_3O_7 + H]^+$ 644.3336, found 644.3326.

4.2.3. Fmoc-Glu-1,4-bisaminomethylbenzene, 3. 2 (96.0 g) was dissolved in a solution (1.5 L) of trifluoroacetic acid/dichloromethane/triisopropylsilane/water (47.5/50/1.25/1.25). The reaction was stirred for 1.5 h at room temperature. The reaction was then concentrated to a volume of 400 mL under reduced pressure and poured into isopropyl ether (1 L). The resulting solid was filtered, washed with isopropyl ether (1 L), and dried under reduced pressure to give **3** (81.9 g). This compound was not purified further and used crude in the next step. ^{1}H NMR (300 MHz, DMSO-d_6): 8.46 (t, 1H, ^3J = 6 Hz), 8.22 (2H, m), 7.90 (d, 2H, ^3J = 7.5 Hz), 7.57 (d, 1H, ^3J = 8.0 Hz), 7.48–7.13 (m, 7H), 4.26 (s, 4H), 3.99 (m, 3H), 2.27 (m, 2H), 1.93 (m, 1H), 1.79 (m, 1H). ^{13}C NMR: 174.3, 172.0, 156.2, 144.3, 141.6, 140.5, 132.9, 129.2, 128.1, 127.7, 127.4, 125.8, 120.6, 66.1, 54.7, 47.1, 42.4, 42.2, 30.7, 27.6. High resolution ESI-TOF-MS: *m*/*z* expected $[C_{28}H_{29}N_3O_5 + H]^+$ 488.2186, found 488.2170.

4.2.4. Boc-Dab(Boc)-OPfp, 4. Boc-Dab(Boc)-OH·DCHA (100 g, 200 mmol) was dissolved in dichloromethane (2 L) at room temperature. Solid pentafluorophenol (36.8 g, 200 mmol) and EDC (38.2 g, 200 mmol) were added. The reaction was stirred at room temperature for 2 h. The resulting solid was filtered and washed with dichloromethane (200 mL). The filtrate was concentrated to a volume of 1 L under reduced pressure, washed with 0.1 N hydrochloric acid (2 × 500 mL), washed with water (500 mL), and washed with brine (500 mL). The organic layer was passed through a plug of silica gel (230 g) and rinsed with dichloromethane (1 L). The filtrate was concentrated to a white glassy solid under reduced pressure to give **4** (86.9 g, 90% yield). ^{1}H NMR (300 MHz, DMSO-d_6): 7.45 (d, 1H, ^3J = 7 Hz), 6.82 (m, 1H), 4.11 (s, 1H), 2.89 (d, 2H, ^3J = 4.5 Hz), 1.70 (m, 2H), 1.17 (s, 9H), 1.14 (s, 9H). ^{13}C NMR: 169.7, 155.9, 142.2, 139.3, 136.2, 125.0, 79.1, 78.0, 51.6, 36.9, 30.7, 28.5. ^{19}F NMR: –149.4 (d, 2F, ^3J = 23 Hz), –154.0 (m, 1F), –158.7 (d, 2F, ^3J = 23 Hz). ESI-MS: *m*/*z* 330.2 [M-2Boc + 2Na]$^+$.

4.2.5. Fmoc-Glu(OH)-1-{4-[Boc-Dab(Boc)-methyl]benzylamide, 5. 3 (81 g, 135 mmol) was dissolved in dimethylformamide (1 L). The pH was adjusted to 7 with diisopropylethylamine (30 mL, 173 mmol). **4** (62 g, 128 mmol) was added to the reaction, and the pH was adjusted to 7 with diisopropylethylamine (10 mL, 57.5 mmol). The reaction was stirred for 2 h. The reaction was monitored by HPLC. The reaction was then poured into water (3.5 L) over 20 min to form a solid. The solid was filtered, washed with water (1 L), and dried under reduced pressure to give **5** (103.9 g). This compound was not purified further and used crude in the next step. ^{1}H NMR (300 MHz, DMSO-d_6): 8.36 (t, 1H, ^3J = 6 Hz), 8.19 (t, 1H, ^3J = 5 Hz), 7.89 (d, 2H, ^3J = 7.5 Hz), 7.74 (d, 2H, ^3J = 7 Hz), 7.59–7.27 (m, 5H), 7.19 (s, 4H), 6.88 (d, 1H, ^3J = 8 Hz), 6.68 (m, 1H), 4.26 (m, 5H), 4.06 (m, 2H), 3.95 (m, 1H), 2.96 (m, 2H), 2.27 (m, 2H), 1.95 (m, 1H), 1.77 (m, 2H), 1.65 (m, 1H), 1.37 (s, 18H). ^{13}C NMR: 174.2, 172.2, 171.8, 156.3, 155.7, 144.2, 141.1, 138.2, 128.0, 127.4, 125.7, 120.5, 78.5, 77.9, 66.1, 54.5, 47.1, 42.2, 37.74, 30.7, 28.6, 28.5, 27.7. High resolution ESI-TOF-MS: *m*/*z* expected $[C_{42}H_{53}N_5O_{10} + H]^+$ 788.3871, found 788.3641.

4.2.6. Fmoc Glu(Rink Amide MBHA resin)-1-{4-[Boc-Dab(Boc)-methyl]benzylamide, 6. Rink Amide MBHA resin (31.25 g, 20 mmol, 0.64 mmol/g) was washed with dimethylformamide (2 × 300 mL). The resin was suspended in 20% piperidine in dimethylformamide (300 mL) and shaken for 1 h. The resin was then filtered, washed with dimethylformamide (2 × 300 mL), dichloromethane (2 × 300 mL), and dimethylformamide (2 × 300 mL). **5** (31.5 g, 40 mmol) and 1-hydroxybenzotriazole (5.4 g, 40 mmol) were dissolved in dimethylformamide (300 mL) and added to the resin. 1,3-Diisopropylcarbodiimide (6.19 mL, 40 mmol) was added, and the reaction was shaken for 2 days at room temperature. The reaction was then filtered and washed with dimethylformamide (1 × 300 mL), dichloromethane (2 × 300 mL), and dimethylformamide (3 × 300 mL). A solution (300 mL) of 5% acetic anhydride and 6% diisopropylethylamine in dimethylformamide was added, and the reaction was agitated for 1 h. The resin was then filtered and washed with dimethylformamide (1 × 300 mL), dichloromethane (2 × 300 mL), and dimethylformamide (3 × 300 mL) to give **6**.

4.2.7. Boc-Dab(Boc)-Tyr(*t*Bu)-dGlu(O*t*Bu)-Cys(Trt)-Hyp-(*t*Bu)-3ClTyr-Gly-Leu-Cys(Trt)-Tyr(*t*Bu)-Ile-Glu(Rink Amide MBHA resin)-1-{4-[Boc-Dab(Boc)-methyl]-benzylamide, 7. The following general procedure was used to attach each subsequent amino acid. The resin was washed with dimethylformamide (2 × 300 mL). 20% Piperidine in dimethylformamide (300 mL) was added, and the resin was agitated for 1 h. The resin was then washed with dimethylformamide (2 × 300 mL), dichloromethane (2 × 300 mL), and dimethylformamide (2 × 300 mL). The amino acid (40 mmol) and 1-hydroxybenzotriazole (5.4 g, 40 mmol) were dissolved in dimethylformamide (300 mL) and added to the resin. 1,3-Diisopropylcarbodiimide (6.19 mL) was added, and the reaction was agitated for 18 h. The resin was then filtered and washed with dimethylformamide (1 × 300 mL), dichloromethane (2 × 300 mL), and dimethylformamide (3 × 300 mL). This procedure was repeated for each amino acid in the following order: Fmoc-Ile-OH, Fmoc-Tyr(*t*Bu)-OH, Fmoc-Cys(Trt)-OH, Fmoc-Leu-OH, Fmoc-Gly OH, Fmoc-Tyr(3-Cl)-OH, Fmoc-Hyp(*t*Bu)-OH, Fmoc-Cys(Trt)-OH, Fmoc-D-Glu(O*t*Bu)-OH, Fmoc-Tyr(*t*Bu)-OH, and Boc-Dab(boc)-OH. The elongated peptide on the resin was dried under reduced pressure to give compound **7**.

4.2.8. L-2,4-Diamino-*N*-butyramide-[Tyr-dGlu-Cys-Hyp-Tyr(3-Cl)-Gly-Leu-Cys-Tyr-Ile-Gln-1-{4-[(L-2,4-diamino-butyrylamino)-methyl]-benzylamide}, 8. 7 (83.18 g) was washed with dichloromethane (3 × 300 mL). The resin was suspended in a solution (1.25 L, 15 mL/g of resin) of trifluoroacetic acid, triisopropylsilane, 1-dodecanethiol, dichloromethane, and water (80:5:5:5:5). The mixture was agitated for 1.25 h. The peptide resin was filtered and washed with trifluoroacetic acid (2 × 100 mL). The filtrate was poured into isopropyl ether (4 L). The resulting solid was washed with isopropyl ether (2 × 600 mL) and acetonitrile (1 × 600 mL). The solid was dried under reduced pressure. The solid was washed with acetonitrile (2 × 200 mL) and dried under reduced pressure to give crude **8** (40.03 g, 92% yield). ESI-MS: *m*/*z* 1719.5 $[M + H]^+$.

4.2.9. L-2,4-Diamino-*N*-butyramide-[Tyr-dGlu-Cys-Hyp--Tyr(3-Cl)-Gly-Leu-Cys-Tyr-Ile-Gln cyclic (2 → 8) disulfide]-

1-{4-[(L-2,4-diamino-butyrylamino)-methyl]-benzylamide}, 9. **8** (40.03 g) was dissolved in a solution (3150 mL) of dimethylsulfoxide, acetonitrile, and water (15:10:75). The reaction was stirred for 24 h at room temperature. The reaction was then diluted with water (3150 mL). The solution was divided in equal portions of 500 mL. 500 mL of solution were injected directly onto a reversed prep HPLC column (Kromasil C18, 100 Å, 10 μm, 5 cm × 25 cm) equilibrated with 95:5 of the following mobile phase (A: 0.1% trifluoroacetic acid in water, B: 0.1% trifluoroacetic acid in acetonitrile). Starting conditions were held for 5 min before initiating the gradient which was 5% to 20% B over 5 min, then 20% to 35% B over 25 min followed by a 3 min ramp to 95% B and wash for 10 min followed by re-equilibration at 5% B for 10 min. Flow rate was 100 mL/min and peaks were detected at 220 nm. Fractions with a purity greater than 98.5% purity were combined and lyophilized to give compound **9** (16.83 g, 97.1% purity, 34% yield (based on peptide content)). High resolution ESI-TOF-MS: *m/z* expected $[C_{78}H_{109}ClN_{18}O_{20}S_2 + H]^+$ 1717.7274, found 1717.6541. ^{1}H, ^{13}C, and ^{15}N chemical shifts of all residues were assigned by means of 2D COSY and HSQC spectra at 9.4T (see Supporting Information Tables S3 and S4 for list of shifts). NOESY spectra yielded more than 90 contacts between adjacent amino acids and confirm the peptide sequence as shown in Figure 1C.

4.2.10. 2-(*R*)-(4,7,10-Tris-*tert*-butoxycarbonylmethyl-1,4,7,10-tetraazacyclododec-1-yl)-pentanedioic Acid, 1-*tert*-Butyl-5-pentafluorophenyl Ester, DOTAGA(O*t*Bu)$_4$-OPfp, 10. The activated ester of the protected DOTAGA ligand (**10**) was synthesized as described previously.[34] 2-(*R*)-2-(4,7,10-Tris-*tert*-butylcarboxymethyl-1,4,7,10-tetraazacyclododec-1-yl)-pentanedioic acid 1-*tert*-butyl ester (DOTAGA(O*t*Bu)$_4$-OH) (29.3 g, 29.4 mmol)[32,34] and pentafluorophenol (8.7 g, 47.3 mmol) were dissolved in dichloromethane (500 mL). Polystyrene-carbodiimide (PS-DCC; 41.2 g, 47.3 mmol; 1.23 mmol/g loading capacity) was added, and the reaction was shaken on an orbital shaker for 3 h. The reaction was monitored by HPLC. The resin was filtered and rinsed with methylene chloride (200 mL). The filtrate was evaporated under reduced pressure. The glassy solid was dried under reduced pressure to give **10** (30.9 g, 85% yield; excess pentafluorophenol will not react in the next step). ESI-MS: *m/z* 867.3 $[M + H]^+$.

4.2.11. L-2,4-[[(1-(1-Carboxy-3-carboxypropyl)-4,7,10-(tris-*tert*-butoxycarbonylmethyl)-1,4,7,10-tetraazacyclodecane)]-butyramide]-[Tyr-dGlu-Cys-Hyp-Tyr(3-Cl)-Gly-Leu-Cys-Tyr-Ile-Gln cyclic (2 → 8) disulfide]-1-{4-[(L-2,4-)-[[(1-(1-carboxy-3-carboxypropyl)-4,7,10-(tris-*tert*-butoxycarbonylmethyl)-1,4,7,10-tetraazacyclodecane)]methyl]benzylamide}, 11. Peptide **9** (11.83 g, 6.89 mmol) was dissolved in dimethylformamide (325 mL). DOTAGA(O*t*Bu)$_4$-OPfp (23.9 g, 27.6 mmol) was added as a solid to the reaction. The pH was adjusted to 6.5 with diisopropylethylamine (6.5 mL). The reaction was stirred at room temperature for 1 h. To the reaction mixture was added additional DOTAGA(O*t*Bu)$_4$ (3.1 g, 3.6 mmol). The pH was adjusted to 6.5 with diisopropylethylamine (1.5 mL), and the reaction was stirred for 0.5 h at room temperature. To the reaction was added additional DOTAGA(O*t*Bu)$_4$ (1.4 g, 1.6 mmol). The pH was adjusted to 6.5 with diisopropylethylamine (1.0 mL), and the reaction was stirred for 0.5 h at room temperature. To the reaction was added additional DOTAGA(O*t*Bu)$_4$ (0.4 g, 0.46 mmol). The pH was adjusted to 6.5 with diisopropylethylamine (0.5 mL), and the reaction was stirred for 1 h. The reaction was monitored by HPLC. Saturated sodium chloride (800 mL) was added to the reaction over 30 min at room temperature, and a solid precipitated. The suspension was stirred for an additional 30 min at room temperature. The solid was filtered, washed with water (500 mL), and dried under reduced pressure to give compound **11** (30.6 g, 100% yield) as an off-white solid. ESI-TOF-MS: *m/z* expected $[C_{218}H_{357}ClN_{34}O_{56}S_2,+,2H]^{2+}$ 2224.8091, found 2224.8091.

4.2.12. L-2,4-[[(1-(1-Carboxy-3-carboxypropyl)-4,7,10-(carboxymethyl)-1,4,7,10-tetraazacyclodecane)]-butyramide]-[Tyr-dGlu-Cys-Hyp-Tyr(3-Cl)-Gly-Leu-Cys-Tyr-Ile-Gln cyclic (2 → 8) disulfide]-1-{4-[(L-2,4-)-[[(1-(1-carboxy-3-carboxypropyl)-4,7,10-(carboxymethyl)-1,4,7,10-tetraazacyclodecane)]methyl]benzylamide}, 12. The *tert*-butyl esters were removed by dissolving **11** (30.6 g, 6.9 mmol) in a cocktail of trifluoromethanesulfonic acid, methanesulfonic acid, 1-dodecanethiol, and water (91.6:2.8:2.8:2.8, 500 mL) at room temperature. The reaction was stirred for 1 h and monitored by HPLC. Cold ethyl acetate (1.25 L) was added, and a solid precipitated. The mixture was stirred for 15 min. The solid was filtered, washed with ethyl acetate (2 × 250 mL), and dried under reduced pressure to give compound **12** (24.4 g, 100% yield) as an off-white solid. ESI-TOF-MS: *m/z* expected $[C_{154}H_{229}ClN_{34}O_{56}S_2 + H + Na]^{2+}$ 1786.7589, found 1786.9338, expected $[C_{154}H_{229}ClN_{34}O_{56}S_2+2Na]^{2+}$ 1797.7521, found 1797.9050.

4.2.13. L-2,4-[Gadolinate(1-), aqua[[(1-(1-carboxy-3-carboxypropyl)-4,7,10-(carboxymethyl)-1,4,7,10-tetraazacyclodecane), monosodium]]-butyramide]-[Tyr-dGlu-Cys-Hyp-Tyr(3-Cl)-Gly-Leu-Cys-Tyr-Ile-Gln cyclic (2 → 8) disulfide]-1-{4-[(L-2,4-)-[Gadolinate(1-), aqua[[(1-(1-carboxy-3-carboxypropyl)-4,7,10-(carboxymethyl)-1,4,7,10-tetraazacyclodecane), monosodium]]methyl]-benzylamide}, EP-2104R. The ligand **12** (24.4 g, 6.9 mmol) was added in portions to a solution of water (500 mL) at room temperature, while maintaining a pH of 6.5 using 1 N sodium hydroxide (277 mL total). Gadolinium(III) chloride hexahydrate ($GdCl_3 \cdot 6H_2O$) (9.8 g, 26.4 mmol) was added to the solution, and the pH was adjusted to 6.5 with 1 N sodium hydroxide (57 mL). The reaction was stirred for 1 h at room temperature. The reaction was monitored by HPLC. Residual gadolinium(III) chloride was neutralized with ethylenediaminetetraacetic acid (EDTA) (10 mL, 1 mmol). The reaction was stirred for 15 min, and the pH was adjusted to 6.5 with 1 N sodium hydroxide (3 mL). The neutralization was monitored by testing with xylenol orange. The product was isolated from solution and purified by reversed phase chromatography. The solution (850 mL) was divided into five equal 170 mL portions. Each portion was injected onto the column (C4 Kromasil, 100 Å, 10 μm, 5 cm × 25 cm) with acetonitrile/water (2:98). Starting conditions were held for 5 min before the gradient was started which was 2% to 18% acetonitrile (ACN) over 25 min, then 18% to 50% ACN over 1 min followed by a 7 min ramp to 80% ACN and wash for 3 min followed by re-equilibration at 2% ACN. Flow rate was 100 mL/min, and peaks were detected at 220 nm. The purified fractions were analyzed by HPLC. Fractions > 95% purity were combined and lyophilized to give EP-2104R (21.5 g, >98% purity by analytical HPLC (see below for method), 4.28 mmol, 62.1% yield from the peptide) as a white powder. ESI-TOF-MS: *m/z* expected $[C_{154}H_{212}ClGd_4Na_5N_{34}O_{56}S_2 + H + Na]^{2+}$ 2151.5173, found 2151.5958, expected $[C_{154}H_{212}ClNa_5N_{34}O_{56}S_2 + 2Na]^{2+}$ 2162.5082, found 2162.5650. UV: λ (ϵ) 192 nm (327 000 cm^{-1} M^{-1}), 219 nm (60 600 cm^{-1} M^{-1}), 277 nm (5700 cm^{-1} M^{-1}). Chiral amino acid analysis[35] showed all amino acids were >99.5% in the L form except Glu which was analyzed as 49.7% D-Glu. This is expected from the D-Glu in the molecule and the L-Gln which is hydrolyzed to Glu in the analytical method.

4.3. LC-MS of EP-2104R and its Disulfide Reduced Product. EP-2104R was analyzed using a Waters Capillary HPLC (30 °C, 15 μL/min, Thermo-Keystone HyPurity C18, 150 mm × 0.5 mm, 3 μm, 0.2 μL injection) with UV (220 nm) detection connected to a Waters (Micromass) Quattro LC mass spectrometer (a triple quadrupole MS) using a gradient method. Mobile phase A was 50 mM ammonium formate, pH 6.8. Mobile phase B was 90% acetonitrile and 10% mobile phase A. Starting from 5% B, the fraction of B increased to 50% over 20 min and was held for 2 min. After a 1 min ramp down to 5% B, the system re-equilibrated at 5% B over 7 min (total time = 30 min). EP-2104R elutes at 14.5 min. The disulfide bond was reduced by treating 90 μL of a 1.2 mM EP-2104R solution with 10 μL of a 200 mM tris(carboxy-

ethyl)phosphine (TCEP) hydrochloride solution in a HPLC vial and allowing the reduction to proceed for 30 min at room temperature. LC-MS of the reduced EP-2104R elutes at 13.1 min with a +2 a.m.u mass shift (see Supporting Information Figure S1).

4.4. NMR Experiments. EP-2104R-La was synthesized in a similar manner as that for EP-2104R, with the exception that $LaCl_3$ was used in place of $GdCl_3$ (Scheme 2). LC/MS analysis indicated that EP-2104R-La was 93.5% pure. About 30 mg of lyophilized EP-2104R-La were dissolved in 600 μL of a solvent mixture comprised of 100 μL of D_2O (Aldrich) and 500 μL of H_2O and transferred into a 5 mm NMR sample tube (Wilmad).

Experiments were performed at 300 K on a Bruker Avance-II 400 MHz spectrometer using an inverse triple channel ($^1H/^{13}C/^{15}N$) probe. Initial 1D ^1H spectra (Figure 1) were taken to optimize experimental parameters such as the proton frequency for water suppression by means of presaturation.[62] The ^1H chemical shift of all spectra has been referenced to DSS (2,2-dimethyl-2-silapentane-5-sulfonic acid). Phase-sensitive gradient-enhanced $^1H-^1H$ COSY, TOCSY (80 ms MLEV-17 spinlock), and NOESY spectra[36] were recorded with a spectral width of 12.25 ppm and 512 increments in t_1 with 16 averaged transients per increment using the watergate pulse sequence for water suppression. NOESY experiments were recorded at mixing times between 80 and 300 ms. All 2D data sets were processed using NMRPipe[63] and subsequently analyzed with SPARKY version 3.106.[64]

4.5. Inertness of EP-2104R and Comparison to Commercial Contrast Agents. MS-325-L solutions at 5 and 20 mM were prepared in 50 mM citrate buffer at pH 3.0, 4.0, and 5.0. The MS-325-L concentration was determined by absorbance at 280 nm and comparison to a standard curve generated by a series of MS-325 solutions of known concentration. A 5 mM solution of EP-2104R was prepared in 50 mM citrate buffer at pH 3.0, 4.0, and 5.0. For a given pH (3, 4, or 5), 1.0 mL of the 20 mM MS-325-L solution was vigorously mixed with 1.0 mL of the 5 mM EP-2104R solution. A 50 μL aliquot was removed for HPLC analysis as described below, and the remainder of the solution was incubated at 60 °C. A 50 μL aliquot was removed and analyzed at 24, 48, 72, and 96 h.

For each of the commercial agents, $[Gd(DTPA)]^{2-}$, [Gd(HP-DO3A)], and [Gd(DTPA-BMA)], a 10 μL aliquot of the 500 mM contrast agent solution was added to 1.0 mL of 5 mM MS-325-L at pH 3.0 or 5.0. After vigorous mixing, a 50 μL aliquot was removed for HPLC analysis as described below and the remainder of the solution incubated at 60 °C. A 50 μL aliquot was removed and analyzed at 10 min intervals out to 40 min after mixing. The [Gd(HP-DO3A)] solution was further sampled at 50 min, 60 min, and then at 4 to 12 h intervals out to 48 h of incubation. The total gadolinium in all solutions was measured by ICP-MS. To control for sample degradation, individual MS-325-L, EP-2104R, $[Gd(DTPA)]^{2-}$, [Gd(HP-DO3A)], and [Gd(DTPA-BMA)] solutions were incubated at 60 °C and analyzed.

The EP-2104R/MS-325-L solutions were analyzed by HPLC (37 °C, 0.8 mL/min, Kromasil C4, 250 mm × 4.6 mm, 5 μL injection) with UV (220 nm) detection using a gradient method. Mobile phase A was 100 mM ammonium phosphate, pH 6.5 plus 200 μM Na_2H_2EDTA. Mobile phase B was 60% acetonitrile and 40% mobile phase A. Starting from 20% B, the fraction of B increased to 32% over 10 min and then from 32 to 50% B over 25 min. After a 30 s ramp to 80% B, the system re-equilibrated at 20% B over 6.5 min (total time = 42 min).

The other solutions were analyzed by HPLC (37 °C, 1.0 mL/min, Zorbax C8, 150 mm × 4.6 mm, 2 μL injection) with UV (220 nm) detection using an isocratic (20% acetonitrile, 80% mobile phase A from above) method for 8 min. This method separates MS-325 from MS-325-L while the other species elute in the void volume.

4.6. Preparation of Fibrinogen. Fibrinogen was dissolved in H_2O or TBS buffer, pH 7.4 and dialyzed in a Slyde-a-Lyzer (10 000 MWCO, Pierce Chemical Co.) vs TBS containing 5 mM citrate at 4 °C. After two changes of buffer, the fibrinogen was centrifuged (10 min, 2000 × g) to remove undissolved material. Fibrinogen concentration was determined by measuring the absorbance at 280 nm (A_{280}), after dilution into TBS, pH 7.4. A 1 mg/mL fibrinogen solution has an absorbance of 1.512 OD units.[65]

Stock fibrinogen solutions ranged in concentration from 10 to 20 mg/mL. Based on the concentration determined postdialysis and the initial mass of the fibrinogen used, the fibrinogen content of the solid commercial material could be calculated. Typically this was about 30% by weight.

4.7. Functional Fibrinogen Concentration in Plasma. The concentration of fibrinogen that is competent to form a fibrin clot was determined by a thrombin clotting time assay against a certified standard using a fibrinogen test kit (Cat. No. 886-A; Sigma Diagnostics). The kit included a 2.52 mg/mL fibrinogen standard, Thrombin (75 U/mL), and imidazole (Im) buffer (30 mM imidazole, 130 mM NaCl, pH 7.35). Clotting times were recorded on an Amelung KC1A Micro Coagulometer. To determine fibrinogen concentration, [Fgn], in the plasma, the standard was diluted in Im to concentrations of 0.50, 0.252, 0.168, 0.126, and 0.084 mg/mL. The sample (150 μL) was added to an Amelung KC1A/KC4A microcuvette and incubated at 37 °C. A 50 μL aliquot of thrombin was added, and the clotting time (TT) was recorded. Plasma samples of unknown concentration were diluted into a linear range (10-fold) in Im, and clotting times were recorded following thrombin addition. The TT of the unknown was used to extrapolate the fibrinogen concentration of the unknown from a linear least-squares fit plot of the log(TT) vs log([Fgn]) data obtained for the standard.

4.8. EP-2104R Sample Preparation. EP-2104R stock solutions (1–10 mM) were prepared by dissolving solid EP-2104R in water. The concentration was determined by gadolinium analysis using ICP-MS. All solutions were prepared by weight. Gadolinium concentrations were calculated based on the concentration of the stock solution and appropriate dilution factors.

Samples in TBS were prepared by mixing appropriate amounts of EP-2104R stock solution and TBS buffer to a final volume of 200 μL. Samples in fibrinogen were prepared by mixing appropriate amounts of EP-2104R stock solution, fibrinogen stock solution, and TBS buffer to a final volume of 200 μL and final fibrinogen concentration of 10 mg/mL. Samples in fibrin gels were prepared by mixing appropriate amounts of EP-2104R stock solution, fibrinogen stock solution, and TBS buffer to a final volume of 200 μL and final fibrinogen concentration of 10 mg/mL. To these solutions was first added a 4 μL aliquot of 2 M $CaCl_2$ followed by 2 μL aliquot of thrombin (0.6 U). The sample was vigorously mixed for 3 s and then allowed to stand at room temperature for 20 min as the fibrinogen polymerized to fibrin and the solution became a gel. For the samples in human plasma, first a stock solution of EP-2104R in fibrinogen enriched plasma was prepared. The relaxivity samples were prepared by mixing appropriate amounts of the EP-2104R/plasma stock with appropriate amounts of fibrinogen enriched plasma to a total volume of 200 μL. The plasma gels (clots) were prepared by taking the plasma samples after measuring the T_1 and T_2 data and then adding first 4 μL of 2 M $CaCl_2$ followed by 2 μL of thrombin (0.6 U). The sample was vigorously mixed for 3 s and then allowed to stand at room temperature for 20 min as the fibrinogen polymerized to fibrin and the solution became a gel.

(62) Neuhaus, D.; Williamson, M. P. *The Nuclear Overhauser Effect in Structural and Conformational Analysis*; 2nd ed.; Wiley-VCH: New York, 2000.
(63) Delaglio, F.; Grzesiek, S.; Vuister, G. W.; Zhu, G.; Pfeifer, J.; Bax, A. *J. Biomol. NMR* **1995**, *6*, 277–93.
(64) Goddard, T. D.; Kneller, D. G.; *SPARKY 3.106*; University of California, San Francisco, Available online at http://www.cgl.ucsf.edu/home/sparky/manual/.
(65) Ugarova, T. P.; Budzynski, A. Z. *J. Biol. Chem.* **1992**, *267*, 13687–93.

4.9. Binding of EP-2104R to Human Plasma Clots. A 10 mM EP-2104R solution was diluted 100-fold with human plasma to give a EP-2104R/plasma stock solution that was 100 μM. Diluting this solution with citrated human plasma resulted in a series of solutions where the total EP-2104R concentration varied between 0.6 and 36 μM. An aliquot of each of these solutions was removed to determine $[EP\text{-}2104R]_{total}$ by ICP-MS. Calcium chloride (2 M) and thrombin were added to yield final concentrations of 10 mM $CaCl_2$ and 1 U/mL thrombin in order to induce clotting. To minimize dilution, small volumes of these reagents (1.7% total volume) were added. The plasma clots were incubated for 1 h at 37 °C in a temperature controlled incubator. The samples were removed individually, and the supernatant was quickly recovered by vigorously stirring the clot with a pipet tip while aspirating the released liquid. About half of the clot volume was recovered from each clot, this was assayed for Gd content by ICP-MS to give $[EP\text{-}2104R]_{free}$.

4.10. Dried Fibrin Plate Preparation. Plasminogen-depleted fibrinogen from human plasma (Calbiochem Cat No.341578) was dialyzed against 50 mM Tris, pH 7.4, 150 mM sodium chloride, 5 mM sodium citrate (TBS·citrate) prior to use. The fibrinogen concentration was adjusted to 5 mg/mL, and $CaCl_2$ was added (7 mM). The fibrinogen solution (50 μL) was dispensed into the wells of a 96-well polystyrene microplate (Immulon-II). A solution (50 μL) of human thrombin (2 U/mL) in TBS was added to each well to clot the fibrinogen and to yield a final fibrin concentration close to 2.5 mg/mL. In one of the assays, fibrin plates were formulated at 1.25 mg/mL. The plates were incubated at 37 °C and evaporated to dryness overnight. The plates were sealed with tape and stored at −20 °C until use. The extent of fibrinogen polymerization (clottability) of individual fibrinogen batches was determined by first measuring the absorbance at 280 nm of the fibrinogen solutions ($A^{pre}{}_{280}$). An aliquot of the fibrinogen solution was then clotted by addition of 1 U/mL thrombin, incubated at 37 °C for 1 h, and then centrifuged to separate the clot. The absorbance of the supernatant ($A^{post}{}_{280}$) was measured. The percent clottability is given by

$$\%C = \left(1 - \frac{A_{280}^{post}}{A_{280}^{pre}}\right) \times 100\% \quad (7)$$

The fibrin concentration, [fbn] (μM), in the plate was calculated from [Fgn] using a molecular weight of 340 kD for fibrin(ogen), as follows:

$$[Fbn] = \frac{\%C\,[fgn]}{100\ 0.34} \quad (8)$$

Solutions of EP-2104R (10 μM and 100 μM) were prepared from a 1 mM stock solution by serial 1:10 dilutions into human plasma. The plasma was treated with 10 μM PPACK, an irreversible thrombin inhibitor, to prevent clotting from residual thrombin present in the fibrin plates. Assayed solutions ranged from $0.4\ \mu M \leq [EP\text{-}2104R]_{total} \leq 52\ \mu M$, and aliquots were taken for ICP determination of $[EP\text{-}2104R]_{total}$. The EP-2104R solutions (100 μL) were added to duplicate wells of the dried fibrin microtiter plate, and the plate was shaken for 2 h. After incubation, solution was removed and the concentration of unbound EP-2104R, $[EP\text{-}2104R]_{free}$, was determined by ICP-MS.

4.11. Relaxation Rate Measurements. Relaxation rates were measured at 20 MHz (0.47 T) and 60 MHz (1.41 T) using a Bruker NMS 120 minispec and a Bruker mq60 minispec, respectively. Samples, 200 μL, were pipetted into glass vials. All samples were equilibrated for at least 20 min at 37 °C and measured at 37 °C. The fibrin gels were prepared in the tube by addition of 4 μL of 2 M $CaCl_2$ and 2 μL of 100 U/mL thrombin solution to a solution already containing EP-2104R and fibrinogen (30 μM), followed by rapid mixing and then equilibration at room temperature for at least 30 min. T_1 was measured with an inversion–recovery pulse sequence.[66] Typically 10–20 spectra were acquired with differing delay times. The preacquisition delay was always set to at least $5T_1$. T_2 was measured using a Carr−Purcell−Meiboom−Gill sequence with 300 to 500 echoes collected.[66] Error in T_1 and T_2 was estimated to be ±5%.[67]

^{1}H nuclear magnetic relaxation dispersion (NMRD) measurements were recorded on a field cycling relaxometer[68] over the Larmor frequency range 0.01 to 50 MHz on 600 μL samples. A total of 22 data points were collected for each dispersion. NMRD were recorded at 5, 15, 25, and 35 °C.

Acknowledgement Acknowledgement is made to John Amedio and Phil Graham for useful discussions and to Frank Qi and Steve Witowski for analytical support.

Supporting Information Available: LC-MS data for EP-2104R and its reduced form; ^{1}H, ^{13}C, and ^{15}N chemical shifts for peptide tetraamine **9** and EP-2104R-La. This material is available free of charge via the Internet at http://pubs.acs.org.

JA800834Y

(66) Braun, S.; Kalinowski, H.-O.; Berger, S. *150 and More Basic NMR Experiments*; Wiley-VCH: Weinheim, 1998.
(67) Pitner, T. P.; Whidby, J. F. *Anal. Chem.* **1979**, *51*, 2203–6.
(68) Koenig, S. H.; Brown, R. D., III *Prog. Nucl. Magn. Reson. Spectrosc.* **1990**, *22*, 487–567.